Electrostatic-Undulatory Theory of Plectonemically Supercoiled DNA

Job Ubbink and Theo Odijk
Faculty of Chemical Engineering and Materials Science, Delft University of Technology, 2600 GA Delft, the Netherlands

ABSTRACT We present an analytical calculation of the electrostatic interaction in a plectonemic supercoil within the Poisson-Boltzmann approximation. Undulations of the supercoil strands arising from thermal motion couple nonlinearly with the electrostatic interaction, giving rise to a strong enhancement of the bare interaction. In the limit of fairly tight winding, the free energy of a plectonemic supercoil may be split into an elastic contribution containing the bending and torsional energies and an electrostatic-undulatory free energy. The total free energy of the supercoil is minimized according to an iterative scheme, which utilizes the special symmetry inherent in the usual elastic free energy of the plectoneme. The superhelical radius, opening angle, and undulation amplitudes in the radius and pitch are obtained as a function of the specific linking difference and the concentration of monovalent salt. Our results compare favorably with the experimental values for these parameters of Boles et al. (1990. *J. Mol. Biol.* 213:931–951). In particular, we confirm the experimental observation that the writhe is a virtually constant fraction of the excess linking number over a wide range of superhelical densities. Another important prediction is the ionic strength dependence of the plectonemic parameters, which is in reasonable agreement with the results from computer simulations.

GLOSSARY

a	DNA hard-core radius
A	Hamaker constant, scaled by k_BT
b	coupling parameter of harmonic potential
c	concentration of monovalent salt
c_r	coefficient of confinement free energy, confinement in r
c_p	coefficient of confinement free energy, confinement in p
d_p	root mean square undulation in p
d_r	root mean square undulation in r
f	perturbation per unit length of strand
$\mathcal{F}$	total free energy of plectoneme per unit length of strand
$\mathcal{F}_{conf}$	confinement free energy per unit length of strand
$\mathcal{F}_{el}$	undulation-enhanced electrostatic free energy per unit length of strand
$\mathcal{F}_{el,0}$	electrostatic free energy of the nonfluctuating configuration per unit length of strand
$\mathcal{F}_{VdW}$	van der Waals free energy per unit length of strand
g	generalized bending constant
G_p	Gaussian distribution of undulations in p
G_r	Gaussian distribution of undulations in r
h	helical repeat DNA relaxed state
$\mathcal{H}_c$	elastic Hamiltonian
k_B	Boltzmann's constant
Lk	linking number
Lk_0	linking number relaxed state
ΔLk	excess linking number
m_1, m_2	fitting coefficients of the approximation of the electrostatic potential
n_s	number concentration monovalent salt
p	pitch/2π of plectonemic superhelix
P_b	DNA bending persistence length
P_t	DNA torsional persistence length
q	elementary charge
Q_B	Bjerrum length $= q^2/(\epsilon k_BT)$
r	radius of plectonemic superhelix
R_c	radius of curvature in plectonemic configuration
s	contour distance
T	absolute temperature
Tw	twisting number
u	angle of plectonemic rotation
u_r	amplitude of undulation in r
u_p	amplitude of undulation in p
w	dimensionless parameter $= 2\kappa r$
ΔTw	excess twisting number
Wr	writhing number
$\mathcal{W}r$	writhe per unit length of strand of the plectonemic helix
Z	function defined by Eq. 19

Greek symbols

α	plectonemic opening angle; $\beta \equiv 2\alpha$
Γ	gamma function
ϵ	dielectric permittivity of solvent
η	constant in the undulatory entropy accounting for non-Gaussianity
κ^{-1}	Debye length
κ_c	curvature classical plectonemic configuration

Received for publication 17 November 1998 and in final form 9 February 1999.

Address reprint requests to Dr. Theo Odijk, Faculty of Chemical Engineering and Materials Science, Delft University of Technology, P.O. Box 5045, 2600 GA, Delft, the Netherlands. Tel.: 31-71-5145-346; Fax: 31-71-5145-346.

A preliminary version of this paper was presented at the workshop "Structure and Function of DNA: A Physical Approach," September 30–October 5, 1996, Mont Ste.-Odile, France.

0006-3495/99/05/2502/18 $2.00

λ	deflection length
μ	dimensionless parameter $= p^2/4r^2$
ν_{eff}	effective linear charge density of DNA
ξ	Poisson-Boltzmann charge parameter
ρ	distance between two points on the superhelical contour
σ	specific linking difference
τ	inverse plectonemic parameter $= h_0/(4\pi r\lvert\sigma\rvert)$
ϕ	dimensionless distance $= \rho/2r$
ψ	electrostatic potential, scaled by $-q/k_{\text{B}}T$
ψ_1	electrostatic potential, scaled by $-q/k_{\text{B}}T$
Ψ	renormalized potential, scaled by $-q/k_{\text{B}}T$
ω_0	twist rate relaxed DNA
Ω	excess twist

INTRODUCTION

Both the global conformation and the local structure of the DNA double helix depend subtly on applied forces. Entropy, interactions, topological constraints, and external forces are nonlinearly intermingled to various degrees, giving rise to the remarkable structural and functional versatility of the DNA molecule (Bloomfield et al., 1974; Sinden, 1994).

When put under sufficient torsional stress, a closed double-helical chain of DNA will respond by forming superhelical structures that are more or less regular and interwound. In the plectonemic helix (Fig. 1), two strands of the double helix are intertwined, each superhelical strand displaced with respect to the other by half the superhelical pitch. At least two end loops are present, but there may be more loops if branching defects occur.

In the supercoiling of DNA, topology and twist are intimately related. The topology of a complex molecule like DNA, however, gives rise to multifarious phenomena, whose relevance extends well beyond supercoiling alone (Wasserman and Cozzarelli, 1986; Cozzarelli and Wang, 1990; Bates and Maxwell, 1993; Stasiak, 1996). It may bear on both isolated molecules and those in congested states, on the formation of knots (Liu et al., 1981), and on the catenation of rings (Martin and Wang, 1970). Topological constraints may be permanent or may manifest themselves only transiently when obstructions or entanglements diffuse away.

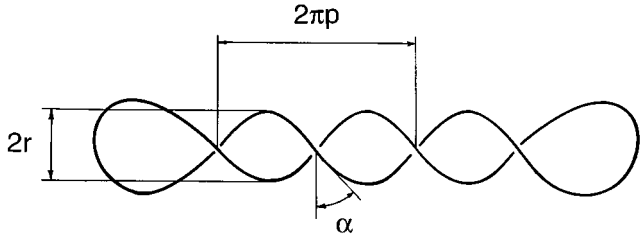

FIGURE 1 A configuration of the plectonemic helix. r is the radius and $2\pi p$ the pitch of the plectoneme, and α is its opening angle.

Our understanding of the biological implications of supercoiling is still incomplete, although many qualitative arguments and models supporting either passive or active roles of supercoiling have been advanced (Sinden, 1987; Cozzarelli and Wang, 1990; Stasiak, 1996). At present it is thought that supercoiling may be functional with respect to the compaction of DNA, in this way enhancing the rate of certain recombination reactions by bringing together distant segments of DNA (Wasserman and Cozzarelli, 1986; Gellert and Nash, 1987) and the regulation of DNA-specific enzymatic activity by a partial unwinding of the double helix, which facilitates a local unstacking of base pairs (Drew et al., 1985).

In other cases, however, supercoiling or the formation of supercoiled domains within a very long DNA molecule may potentially interfere with the proper functioning of the cell. For instance, if the cell were not able to relax excess supercoiling density, both DNA transcription (Liu and Wang, 1987) and the wrapping of DNA into nucleosome core particles (Wolffe, 1992) would be hampered by the accumulation of positive supercoils in the remaining free loops.

In dealing with the myriad topological impediments that occur during normal cell operation, with or without associated elastic stresses, the living cell has at its disposal a complex enzymatic machine, of which the topoisomerases form the center (Wang, 1971, 1991, 1996; Gellert, 1981). Various members of this class of enzymes are able to manipulate the torsional state of the double helix either actively, by introducing twist into the double helix at the expense of the consumption of ATP, or passively, by relaxing the excess twist in the circular DNA. In the latter case the release of excess twist may be the sole driving force of the topological reaction.

The supercoiling of DNA was revealed by electron microscopy after hints of its anomalous behavior in sedimentation experiments (Vinograd et al., 1965). The topology and physical structure of supercoiled DNA have since been studied by a wide variety of techniques, including dynamic light scattering (Langowski et al., 1990), x-ray diffraction (Brady et al., 1987), site-specific recombination and transposition (Boles et al., 1990), microcalorimetry (Seidl and Hinz, 1984), gel electrophoresis (Keller and Wendel, 1974; Keller, 1975; Depew and Wang, 1975; Pulleyblank et al., 1975), dialysis studies of intercalating agents (Bauer and Vinograd, 1970; Hsieh and Wang, 1975), ring closure probabilities (Shore et al., 1981; Shore and Baldwin, 1983), and single-molecule stretching experiments (Strick et al., 1996). Many of these experiments were directed mainly at the elucidation of the topological state itself. Unfortunately, most of the common physical chemical techniques do not allow a precise and unambiguous assignment of supercoil structure because the resolution in the experiments is too weak.

In recent years, however, modern (cryo-) electron microscopic techniques have been applied, aiming at a deeper reassessment of supercoil structure (Boles et al., 1990;

Adrian et al., 1990; Bednar et al., 1994). The supercoil parameters are thus becoming better known, and with greater accuracy. Of course, microscopy remains a technique that is never without some ambiguity.

The correct topological relations governing closed DNA were determined merely a few years after the experimental discovery of DNA supercoiling (White, 1969; Fuller, 1971, 1978; Bauer et al., 1978). The conformations of DNA rings and coils under torsion have been studied primarily within the elastic limit (Fuller, 1971; Camerini-Otero and Felsenfeld, 1978; LeBret, 1979, 1984; Benham, 1979, 1983; Tanaka and Takahashi, 1985; Wadati and Tsuru, 1986; Tsuru and Wadati, 1986; Hao and Olson, 1989; Hunt and Hearst, 1991; Shi and Hearst, 1994; Westcott et al., 1997). An analytical study that goes some way in explaining plectonemic structure is the elastic theory by Hunt and Hearst (1991). They calculated the bulk plectonemic parameters as a function of the excluded-volume radius of the DNA.

The thermally averaged properties of supercoiled DNA have been probed extensively by computer simulations (Vologodskii et al., 1979, 1992; Klenin et al., 1991; Olson and Zhang, 1991; Chirico et al., 1993; Rybenkov et al., 1997; Delrow et al., 1997). The simulations differ widely in their degree of sophistication, but the results are, in general, mutually consistent, and the agreement with experiment is satisfactory in most cases.

The analytical development of the statistical mechanics of supercoiling is hampered considerably by the topological constraints (Shimada and Yamakawa, 1984, 1985; Tanaka and Takahashi, 1985; Benham, 1990; Hearst and Hunt, 1991; Guitter and Leibler, 1992; Marko and Siggia, 1994, 1995; Odijk, 1996). Quantitative understanding was first achieved in the consideration of the ring closure probabilities of short stiff chains with torsion (Shimada and Yamakawa, 1984, 1985). The similarity between a superhelical strand undulating within a supercoil and a wormlike chain confined within a harmonic potential was noted by Marko and Siggia (1994), who advanced a simple scaling picture of supercoil structure in the limit of fairly large fluctuations.

Even for tight bending, it has been argued that the entropy and bending of a wormlike chain are superposable to a good approximation (Marko and Siggia, 1995; Odijk, 1996). This introduces a major shortcut to theoretical work. In fact, a semiclassical treatment of supercoil structure may be put forward. Exploiting the special symmetry inherent in the classical elastic Hamiltonian of the plectoneme, we have recently shown that some of the peculiarities of plectonemic DNA observed both in experiment and in computer simulation may be understood in fairly simple terms (Odijk and Ubbink, 1998).

Besides topology, bending, and entropy, there is a fourth problem that needs to be analyzed, namely the interaction of superhelical DNA with itself. Under physiological conditions, the behavior of DNA is strongly influenced by the screened Coulomb forces exerted by its negative phosphate charges. The electrostatic interaction in supercoiled DNA immersed in a monovalent salt solution has been taken into account via the use of an effective diameter, both in simulations (Vologodskii et al., 1992) and in analytical theory (Marko and Siggia, 1994). The effective diameter depends on the ionic strength of the solution (Onsager, 1949; Stigter, 1977), but it was introduced as a statistical concept pertaining to the isotropic interaction between two straight charged rods. The statistical averaging and Boltzmann weighting are, in principle, entirely different in a theory of supercoils. In recent work the use of an effective diameter was circumvented. A soft, exponentially decaying electrostatic potential was taken into account in computer simulations (Fenley et al., 1994; Vologodskii and Cozzarelli, 1995) and, albeit within a bare, unrenormalized approximation, in analytical theory (Marko and Siggia, 1995). In positionally ordered systems, however, we recall that the bare electrostatic interaction is strongly enhanced by even small undulations of the chains around their equilibrium conformation (Odijk, 1993a). Entropy and electrostatics conspire to give rise to an electrostatic-undulatory interaction.

Here we would like to go beyond previous theoretical work in the following ways: 1) The electrostatics is dealt with by summing all interactions in a far-field Poisson-Boltzmann approximation. Closed analytical approximations for the electrostatic potential at all values of the plectonemic parameters are given, which may also be useful outside the context of this paper. 2) The potentially powerful enhancement of the potential by thermal undulations is computed within a Gaussian ansatz for the undulatory confinement. 3) The pitch and radius are two scales determining a plectonemic supercoil. It will turn out that they cannot be treated on the same footing at all. 4) Analytical procedures are employed to handle the total free energy of the plectoneme (i.e., the sum of electrostatics, entropy, bending, and twisting), so that we attain a tractable theory for supercoiling that is of practical use and yields physical insight at the same time.

The outline of the paper is as follows. First, we recapitulate the main topological relations governing covalently closed circular DNA. We calculate, both numerically and asymptotically, the electrostatic potential exerted by the plectonemic configuration to evaluate the free energy of electrostatic interaction. We next discuss the entropic mechanism by which small undulations of the strands within the supercoil couple nonlinearly with the electrostatic potential and present an approximate calculation of this effect. Then the total free energy of the supercoil is cast in the scheme previously proposed by us (Odijk and Ubbink, 1998). We concentrate on the limit of tight supercoiling, for it is then possible to postulate the existence of semiclassical configurations, in which the undulations are small. The free energy consists of an elastic contribution and a perturbative term, the electrostatic-undulatory interaction. We self-consistently minimize the total plectonemic free energy with the help of the iterative procedure derived by us earlier (Odijk and Ubbink, 1998). Our results are compared with the available quantitative data. Finally, in the Appendices, we give a detailed analysis of an entropic coefficient and

briefly consider the effect of attractive interactions on plectonemic structure.

TOPOLOGY

Even when we disregard the probability of knot formation in the double helix itself, the closure of a double-stranded molecule like DNA can take place in many topologically distinct ways. Either strand closes on itself because the two strands run in opposite directions along the double helix, and the ends of the sugar-phosphate backbones are of a different chemical nature. The number of turns of the strands of the double helix around one another characterizes a specific topological state. For a covalently closed DNA molecule, the appropriate topological invariant is the linking number Lk (Fuller, 1971). Normal B-DNA in the relaxed state forms a right-handed helix characterized by a helical repeat h of ~3.5 nm (or, equivalently, 10.5 bp) (Bates and Maxwell, 1993), so to measure the degree of supercoiling, which may manifest itself in either under- or overwinding of the double helix, it is convenient to introduce the linking number in the relaxed state Lk_0. This number is defined in such way that for B-DNA it is positive (Bauer et al., 1978; Cozzarelli et al., 1990; Bates and Maxwell, 1993).

In 1969 White derived a relation between the linking number and two configurational quantities, one bearing on the local twist of the chain and the other reflecting the global shape of the molecule (White, 1969):

$$Lk = Tw + Wr \tag{1}$$

where Tw is the twisting number, defined by

$$Tw = \frac{1}{2\pi}\oint ds[\omega_0 + \Omega] \tag{2}$$

The integration is performed along the contour of the axis of the double helix, ω_0 is the intrinsic rate of twist of the relaxed double helix, and Ω is the excess twist. The second quantity introduced in Eq. 1 is the writhing number Wr, which, for an arbitrary space curve, is given by the Gauss integral (White, 1969; Călugăreanu, 1959). The writhe is a functional of the configuration of the axis of the double helix only. The energy of a supercoil depends on the twist that can be eliminated via Eq. 1 in favor of the writhe. In this way, the energy conveniently becomes a functional of the configuration vector.

Analytical evaluation of the writhing number is generally cumbersome; simple analytical approximations have been derived in several cases, including that of the regular interwound configuration (Fuller, 1971; White and Bauer, 1986). We will need the writhe per unit length of strand of a plectonemic superhelix,

$$^{\circ}Wr = \pm\frac{p}{2\pi[p^2 + r^2]} \tag{3}$$

In Eq. 3 it is assumed that end loops may be neglected. The plus and minus signs hold for left- and right-handed plectonemic helices, respectively. r is the radius, and $2\pi p$ is the pitch of the superhelix (see Fig. 1); the two variables are assumed to be uniform. The plectonemic opening angle α is defined by $\tan\alpha = p/r$.

Deviations from the relaxed state are measured by the excess linking number $\Delta Lk = Lk - Lk_0$ and the excess twisting number $\Delta Tw = Tw - Lk_0$. The writhe is taken to be zero in the relaxed state. Furthermore, $Lk_0 = 2\pi\omega_0 l/h$, where l is the DNA contour length, so we can write

$$\Delta Lk = \Delta Tw + Wr \tag{4}$$

Both excess quantities may be positive or negative, pertaining either to over- or underwinding of the double helix.

By dividing the excess linking number ΔLk by Lk_0, we obtain the specific linking difference σ:

$$\sigma = \frac{\Delta Lk}{Lk_0} \tag{5}$$

For a homogeneously supercoiled molecule, the degree of supercoiling is determined completely by the intensive quantity σ.

ELECTROSTATIC POTENTIAL OF PLECTONEMIC DNA

We view the double-stranded DNA molecule as a closed circular curve of cylindrical cross section. Its body is a uniform dielectric with a permittivity much lower than that of water, and its surface is assumed to bear a uniform charge density. In aqueous solution, the electrostatic potential of the supercoil is often screened by excess 1:1 salt, so we address its electrostatics within the nonlinear Poisson-Boltzmann approximation. This has been established to be quite accurate (Fixman, 1979).

The difficult problem of solving the Poisson-Boltzmann equation for the charged plectoneme may be replaced by a much simpler one, however. Because the distances between adjacent winds in the plectonemic helix are typically much larger than about twice the sum of the DNA hard-core radius a and the Debye screening length κ^{-1} (owing to Boltzmann weighting), we are interested in the far-field asymptotic solution to the Poisson-Boltzmann equation only. This solution is essentially a linear superposition of effective Debye-Hückel potentials arising from all of the phosphate charges on the DNA supercoil. In the case of a straight polyion, the charged cylinder may be replaced by a line charge coinciding with the axis of the cylinder (Brenner and Parsegian, 1974). The nonlinear screening in the inner double layers of the charged cylinder is taken into account by adjusting the effective charge density ν_{eff} (i.e., the number of charges per unit length along the helical axis) in such a way that the outer double layers of the respective potentials coincide (Stroobants et al., 1986).

Here we consider the potential exerted by a polyion of plectonemic shape, which is again characterized by a radius r and a pitch $2\pi p$ (Fig. 1). Corrections to the effective charge density ν_{eff} due to the superhelical curvature of the polyions may be neglected, for they are of order $(\kappa R_c)^{-2}$ (Fixman, 1982) when the characteristic radius of curvature $R_c \approx (p^2 + r^2)/r$ of the plectoneme is much larger than the Debye length.

Next, we superpose Debye-Hückel potentials exerted by the uniformly charged superhelix, whose charge density along the helical axis is ν_{eff}. We choose a Cartesian coordinate system (x, y, z) in such a way that the z axis coincides with the central axis of the plectonemic helix (Fig. 2). M: $(r, 0, 0)$ is a point on one strand of the plectonemic helix, and N: $(-r\cos u, \pm r\sin u, pu)$ is a point on the opposing strand; the plus and minus signs hold for left- and right-handed superhelices, respectively. u is the parameterization along the plectonemic axis. The distance ρ between M and N may be written as

$$\rho(u) = [2r^2[1 + \cos u] + p^2u^2]^{1/2} \tag{6}$$

The total Debye-Hückel potential exerted by the opposing strand on point M of the test strand is then given by

$$\psi(p, r) = 2\xi \int_0^\infty \mathrm{d}s \frac{\exp[-\kappa\rho]}{\rho}$$

$$= 2\xi[p^2 + r^2]^{1/2} \int_0^\infty \mathrm{d}u \frac{\exp[-\kappa\rho]}{\rho} \tag{7}$$

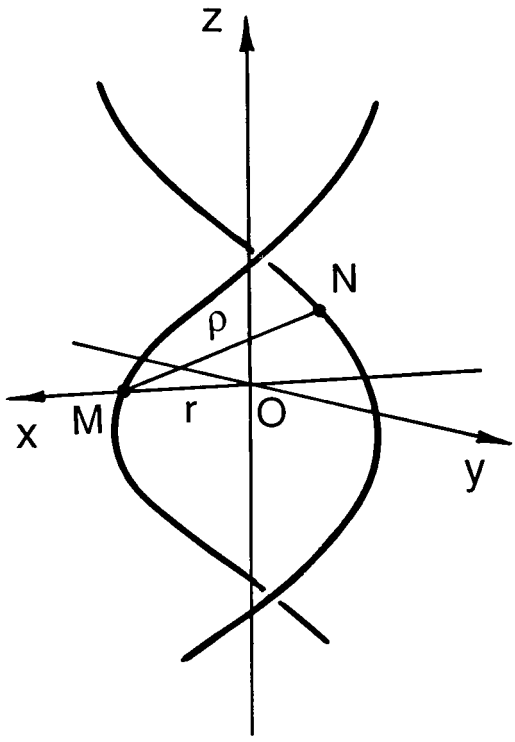

FIGURE 2 The plectonemic coordinate system.

where s is the arclength from $(-r, 0, 0)$ to N along the opposing strand, $\mathrm{d}s = [(p^2 + r^2)^{1/2}/p]\mathrm{d}z$. $\xi \equiv Q_B\nu_{\text{eff}}$ is an effective charge parameter that may be calculated within the Poisson-Boltzmann approximation (Stroobants et al., 1986; Philip and Wooding, 1970), κ^{-1} is the Debye length defined by $\kappa^2 \equiv 8\pi Q_B n_s$, $Q_B \equiv q^2/\epsilon k_B T$ is the Bjerrum length, q is the elementary charge, and n_s is the number concentration of monovalent salt. ϵ is the permittivity of the solvent, k_B is Boltzmann's constant, and T is absolute temperature. In the integrand of Eq. 7 one recognizes the Debye-Hückel potential exerted by an element of arclength, i.e., a Coulomb potential screened by a decaying exponential. The potential has been multiplied by the elementary charge and divided by k_BT to render it dimensionless, for convenience. The electrostatic self-energy of the DNA helix itself will be assumed to be constant.

The potential may be usefully expressed as a function of the two dimensionless variables $w \equiv 2\kappa r$ and $\mu \equiv p^2/4r^2$, so that Eq. 7 is transformed into

$$\psi(w, \mu) = \xi[1 + 4\mu]^{1/2} \int_0^\infty \mathrm{d}u \frac{\exp[-w\phi(u)]}{\phi(u)} \tag{8}$$

with

$$\phi(u) = \left[\frac{1}{2}[1 + \cos u] + \mu u^2\right]^{1/2} \tag{9}$$

To investigate the physical behavior of the potential, we here anticipate that $w \geq 1$ and $4\mu w^2 \geq 1$, for the inner double layers of the strands are unlikely to interpenetrate. We also do not expect twisting forces within the DNA helix to compete with electrostatic forces in the event they become unduly high ($\gg k_BT$/nm) upon such interpenetration.

It is seen from the behavior near $u = 0$ of the integrand in Eq. 8 that the construction of asymptotic expansions for large w that are uniformly valid for all $\mu > 0$ is not standard. Bleistein's method (Olver, 1974) could be used in this case, but the presence of cos u in $\phi(u)$ proves to be awkward. Therefore, we have opted for the usual Laplace method (Olver, 1974; Bender and Orszag, 1978), albeit as it is applied in various regimes, for it does not yield a uniformly valid approximation for integrals of the type in Eq. 8.

For $w \gg 1$, the integrand in Eq. 8 decays exponentially fast away from some minimum $u = u_m$ of the function $\phi(u)$. A major contribution to the integral comes from the neighborhood of u_m, so we expand $\phi(u)$ around u_m:

$$\phi(u) = \phi(u_m) + \frac{1}{k!}(u - u_m)^k\phi^{(k)}(u_m) + \cdots \tag{10}$$

Here we retain only the first nonvanishing term, which is positive. The leading asymptotic contribution to Eq. 8 is then given by (Olver, 1974; Bender and Orszag, 1978)

$$\psi(w, \mu) \sim \frac{c_1\xi[1 + 4\mu]^{1/2}\Gamma(1/k)(k!)^{1/k}}{k\phi(u_m)[w\phi^{(k)}(u_m)]^{1/k}} \exp[-w\phi(u_m)] \tag{11}$$

where $c_1 = 1$ if the minimum is at $u_m = u_0 = 0$ and $c_1 = 2$ if $u_m > 0$ ($m = 1, 2, \ldots$).

The case $1/4w^2 < \mu < 0.2$

We have to distinguish among a number of cases, depending on the value of μ. If $\mu < 1/4$, we have either one or a multiple of local minima, which are to be determined from $\sin u_m/u_m = 4\mu$. In view of our lower bound $\mu > 1/4w^2$, the minima beyond the first may be neglected: this is easily proved by noting that the first minimum $u_1 < \pi$ and $u_m > 2\pi$ ($m = 2, 3, \ldots$) and $w\phi(u_m) \geq u_m/2$. If we approximate $\sin u_1$ by the polynomial $-(4/\pi^2)u_1^2 + (4/\pi)u_1$ (which is reasonable for $\mu < 0.2$), we determine the first minimum to be $u_1 \approx \pi - \pi^2\mu$. The lead term for the potential is then approximately given by

$$\psi(w, \mu) \sim 2\xi\left[\frac{2\pi}{w\phi(u_1)}\right]^{1/2}\left[\frac{1 + 4\mu}{-\cos u_1 + 4\mu}\right]^{1/2} \exp[-w\phi(u_1)] \tag{12}$$

If we now let μ become very small by increasing the radius r while keeping the pitch $2\pi p$ constant ($u_1 \to \pi$), we ultimately obtain the limiting form for the potential, which is independent of r:

$$\psi(w, \mu \ll 1) \approx 2\xi\left[\frac{2}{\kappa p}\right]^{1/2} \exp[-\pi\kappa p] \tag{13}$$

This is interpreted as the potential at the test strand due to two neighboring line charges, each at a distance of half the superhelical pitch. The line charges are effectively straight on the scale of p.

The case $\mu = 1/4$

For μ larger than ~0.2, u_1 starts to approach zero, and this causes problems. In fact, as μ increases to 1/4, Laplace's method fails because the second-order derivative at the minimum becomes small compared to the value of the next nonvanishing derivative, which is of fourth-order. For $\mu \geq 1/4$, $\phi(u)$ attains only one minimum at $u_0 = 0$. The case $\mu = 1/4$ is peculiar, for the first nonvanishing derivative at $u_0 = 0$ is fourth-order. Upon using Eq. 11, we may write for the potential

$$\psi(w, 1/4) \approx \frac{24^{1/4}\Gamma(1/4)\xi}{2w^{1/4}} \exp[-w] \approx 4.012\xi w^{-1/4}\exp[-w] \tag{14}$$

The case $\mu > 1/4$

For $\mu > 1/4$, the second-order derivative again comes into play and dominates the contribution from the fourth-order derivative for large enough μ (the third-order derivative vanishes at $u = 0$ for any μ). For μ somewhat larger than unity, we may again use the Laplace method so as to obtain

$$\psi(w, \mu) \sim \xi\left[\frac{2\pi}{w}\right]^{1/2}\left[\frac{4\mu + 1}{4\mu - 1}\right]^{1/2} \exp[-w] \tag{15}$$

If we let $\mu \to \infty$ by increasing the pitch $2\pi p$ while keeping the radius r constant, Eq. 15 reduces to a limiting form independent of p:

$$\psi(w, \mu \gg 1) \approx \xi\left[\frac{\pi}{\kappa r}\right]^{1/2} \exp[-2\kappa r] \tag{16}$$

This is interpreted as the potential at a test strand exerted by a straight line charge at a distance $2r$. Note the formal equivalence of Eqs. 13 and 16.

We have derived the asymptotic forms of the potential in several regimes to gain physical insight into its dependence on the superhelical pitch angle. Interacting charged rods exert an electric torque on each other, forcing them toward a perpendicular orientation, an effect with measurable impact on various phenomena (Stroobants et al., 1986). In the present analysis (Eqs. 12–16), the influence of twist might appear to be less severe. The simplest uniform approximation—a superposition of the two limiting forms given by Eqs. 13 and 16—seems not such a bad zeroth-order expression at first sight:

$$\psi_0 \approx 2\xi\left[\frac{2}{\kappa p}\right]^{1/2} \exp[-\pi\kappa p] + \xi\left[\frac{\pi}{\kappa r}\right]^{1/2} \exp[-2\kappa r] \tag{17}$$

This was already proposed by Marko and Siggia (1995). See Table 1 for the accuracy of this simple form. Equation 17 becomes fairly poor whenever $w \geq 4$ and $0.1 \leq \mu \leq 1$,

TABLE 1 Electrostatic potential: accuracy of the simple superposition approximation (Eq. 17)

	w					
μ	2		6		10	
0.01	3.614	4.077	0.557	0.583	0.122	0.130
0.1	0.728	0.830	$7.830 \cdot 10^{-3}$	$2.0332 \cdot 10^{-2}$	$1.131 \cdot 10^{-4}$	$5.807 \cdot 10^{-4}$
0.3	0.326	0.431	$2.588 \cdot 10^{-3}$	$5.574 \cdot 10^{-3}$	$3.603 \cdot 10^{-5}$	$8.581 \cdot 10^{-5}$
1	0.244	0.287	$2.537 \cdot 10^{-3}$	$3.183 \cdot 10^{-3}$	$3.599 \cdot 10^{-5}$	$4.566 \cdot 10^{-5}$
3	0.240	0.247	$2.537 \cdot 10^{-3}$	$2.703 \cdot 10^{-3}$	$3.599 \cdot 10^{-5}$	$3.864 \cdot 10^{-5}$
10	0.240	0.234	$2.537 \cdot 10^{-3}$	$2.551 \cdot 10^{-3}$	$3.599 \cdot 10^{-5}$	$3.646 \cdot 10^{-5}$

First number of each entry: Eq. 17. Second number: numerical solution of Eq. 8. $\xi = 1$; $w = 2\kappa r$; $\mu = p^2/4r^2$.

whereas the asymptotic formulas Eqs. 12, 14, and 15 fare much better.

However, the magnitude of the plectonemic potential is, in itself, not such a serious issue. The two major problems with Eq. 17 are, in fact, as follows: 1) We ultimately need to minimize the total free energy of the supercoil, so derivatives are important; the derivative of ψ_0 with respect to p is often a vast underestimate of the actual derivative (see Table 1). 2) Undulation enhancement (as we explain below) of any weak exponential-like term one would inadvertently introduce could lead to a huge (fictive) contribution to the undulatory electrostatic energy. We are therefore forced to devise a bare plectonemic energy considerably more accurate than Eq. 17.

Now it so happens that in practice the superhelical pitch angle is rarely smaller than 45°, i.e., $\alpha \geq 45°$ or $p \geq r$ or $\mu \geq 1/4$. Accordingly, we focus only on regime c as defined above, and the asymptotic form (Eq. 15) suggests an approximation that does not have the unphysical divergence at $\mu = 1/4$:

$$\psi_1 \approx \xi\left[\frac{2\pi}{w}\right]^{1/2} \exp[-w]Z \tag{18}$$

$$Z \equiv 1 + \frac{m_1}{\mu} + \frac{m_2}{\mu^2} \quad (\mu \geq 1/4) \tag{19}$$

We have adjusted the coefficients $m_1 = 0.207$ and $m_2 = 0.054$ to let ψ_1 agree closely with the numerical evaluation ψ_{num} of Eq. 8 (see Table 2). Clearly, the function ψ_1 is accurate enough to circumvent both major difficulties quoted above. Moreover, Eqs. 18 and 19 show that the pitch and radius are definitely not independent variables, as in the superposition formula (Eq. 17). Thus there is a twisting torque of electrostatic origin.

UNDULATION ENHANCEMENT OF THE ELECTROSTATIC INTERACTION

If we were to neglect undulations of the strands, the electrostatic free energy per unit length of strand in the plectonemic supercoil would be calculated by multiplying the effective linear charge density $\nu_{eff} \equiv \xi/Q_B$ of the test strand by the electrostatic potential exerted by its neighbor:

$$\frac{\mathcal{F}_{el,0}}{k_B T} = \frac{1}{2}\,\nu_{eff}\psi_1(2\kappa r, p^2/4r^2) \tag{20}$$

The factor 1/2 has been introduced to avoid double counting.

TABLE 2 Ratio of the approximation ψ_1 (Eq. 18) to the plectonemic electrostatic potential and the numerical calculation ψ_{nm} of Eq. 8

	w		
μ	2	6	10
0.1	2.44	1.057	0.525
0.3	1.27	1.042	0.960
1	1.054	1.005	0.994
3	1.044	1.009	1.001
10	1.047	1.015	1.008

$w = 2\kappa r$; $\mu = p^2/4r^2$.

However, as is already discernible in electron micrographs, the plectonemic helix is definitely perturbed by thermal undulations, which in some cases may be so wild that it becomes impossible to speak of a regular interwound state. Here we restrict ourselves to plectonemic supercoiling at moderate to high values of the specific linking difference so that the superhelix may be viewed as tightly wound. In this limit, the strands in the plectonemic helix are pinned in a deep potential trough, causing the undulations of the strands within the supercoil to remain fairly weak. The slopes of the free energy well in which the strands are undulating are dominated by the electrostatic interaction favoring some optimal pitch and optimal radius, and by the torsional free energy, coming into play via White's relation, which favors an increasing pitch and decreasing radius.

The strands of the plectonemic superhelix are ordered positionally with respect to one another, so we expect undulation enhancement of the interactions to occur, in a manner similar to that conceived earlier for hexagonal phases of semiflexible polyions (Odijk, 1993a). In particular, owing to the exponentially screened form of the electrostatic interaction, we anticipate a strong enhancement of the bare electrostatic interaction by the undulations.

Now, a rigorous analytical treatment of the statistical mechanics of a plectonemic worm interacting with itself is anything but trivial. The typical radius of curvature is much smaller than the persistence length, so we are in the semiclassical limit (Odijk, 1996), where fairly weak undulations of the chains are defined with respect to a (local) state of minimum energy. The latter may be called a classical limit. The configurational statistics of such tightly curved worms has been dealt with by several methods (Shimada and Yamakawa, 1984; Marko and Siggia, 1995; Odijk, 1996). The general conclusion is that a stiff chain undulates virtually independently of its degree of tight bending. We simply assume that this holds true in our case with electrostatics included, despite the lack of a rigorous mathematical proof. Nevertheless, from a physical point of view, switching on repulsive forces does not increase the import of bending; rather the reverse is true. On the whole, we expect the electrostatics to be balanced by entropy as far as the undulations of the plectoneme are concerned. Next, we know the plectoneme fluctuates about some equilibrium configuration. Clearly positional order exists that is similar but not identical to that of a linear polyion undulating within a hexagonal lattice (Odijk, 1993a). One obvious difference is that a plectonemic strand does not undulate within a potential of simple symmetry. At this stage we simply posit a two-variable description (r and p independent) to introduce coarse-grained undulatory electrostatics. Marko and Siggia (1995) have presented arguments based on pseudopotentials

that this is a useful approximation. In this paper we disregard all end effects, including branching.

We now first presuppose that the undulations in both r and p are small. Below, we shall see that we will be forced to modify this hypothesis, but we need to investigate this case first. It is then reasonable to postulate a Gaussian distribution for the undulations in the two-dimensional (r, p)-space:

$$G_r(u_r) = \frac{1}{\pi^{1/2} d_r} \exp\left[-\frac{u_r^2}{d_r^2}\right]$$

$$G_p(u_p) = \frac{1}{\pi^{1/2} d_p} \exp\left[-\frac{u_p^2}{d_p^2}\right] \tag{21}$$

where u_r and u_p and $d_r/2^{1/2}$ and $d_p/2^{1/2}$ are the undulatory amplitudes in r and p and their root mean squares, respectively ($d_r \ll r$, $d_p \ll p$). Orientational fluctuations of neighboring polymer segments may be neglected in this limit (Odijk, 1993a).

The two strands in the plectonemic helix are presumed to undulate independently. Let us choose one of the strands and average its potential over all of the undulations (Fig. 3 *a*):

$$\begin{aligned}
&\Psi(\kappa r, \kappa p) \\
&= \int_{-\infty}^{\infty} du_p \int_{-\infty}^{\infty} du_r G_r(u_r) G_p(u_p) \psi_1(\kappa[r + u_r], \kappa[p + u_p]) \\
&\approx \xi \left(\frac{\pi}{\kappa r}\right)^{1/2} \exp[\kappa^2 d_r^2 - 2\kappa r] \left[Z(\mu) + \frac{d_p^2}{2p^2}\left(\frac{3m_1}{\mu} + \frac{10m_2}{\mu^2}\right)\right] \\
&\quad + \mathbb{O}\left(\frac{1}{\kappa r}\right) + \mathbb{O}\left(\frac{d_p^4}{p^4}\right)
\end{aligned} \tag{22}$$

The bare potential ψ_1 given by Eq. 18 is smeared out by the undulations of the test strand exerting the potential. The renormalization of the radial undulation is potentially strong, for it is exponential. But the renormalization of the longitudinal undulation is slight because the dependence of ψ_1 on p is weak. Equation 22 has been derived using the fact that $d_p \ll p$.

The strand adjacent to the test strand is also undulating (Fig. 3 *b*). Because of symmetry, averaging the renormalized potential (Eq. 22) over the undulations of the adjacent strand is equivalent to averaging again over the undulations of its neighbor:

$$\begin{aligned}
&\frac{\mathcal{F}_{el}}{k_B T} \\
&= \frac{1}{2}\nu_{eff} \int_{-\infty}^{\infty} du_p \int_{-\infty}^{\infty} du_r G_r(u_r) G_p(u_p) \Psi(\kappa[r + u_r], \kappa[p + u_p]) \\
&\approx \frac{\xi^2}{2Q_B}\left(\frac{\pi}{\kappa r}\right)^{1/2} \exp[2\kappa^2 d_r^2 - 2\kappa r] \left[Z(\mu) + \frac{d_p^2}{p^2}\left(\frac{3m_1}{\mu} + \frac{10m_2}{\mu^2}\right)\right]
\end{aligned} \tag{23}$$

$\mathcal{F}_{el}$ is the free energy of electrostatic interaction per unit length of strand. In Eq. 23 relative terms of $\mathbb{O}(1/\kappa r)$ and $\mathbb{O}(d_p^4/p^4)$ have been consistently deleted.

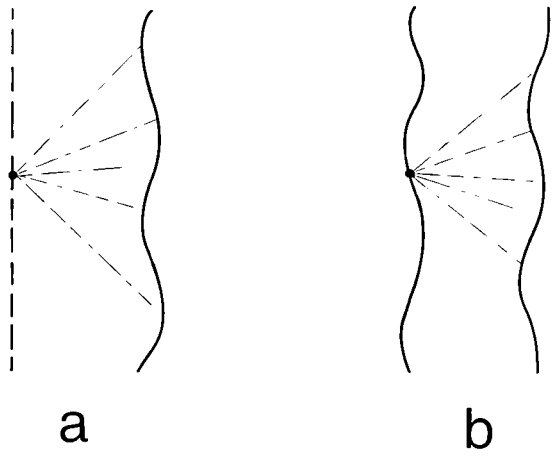

FIGURE 3 The bare electrostatic potential within the plectonemic configuration (r, p) is averaged over all undulations of (*a*) the strand adjacent to the test strand and (*b*) the test strand itself.

ENTROPY

In the previous section we discussed the mechanism by which small undulations of magnitudes d_r and d_p of the strands within the plectonemic superhelix give rise to an amplification of the bare electrostatic interaction that is weighted unevenly. Now, the reduction of entropy of a worm upon confinement to the close neighborhood of its classical path—the typical transverse wanderings being of average amplitude d—is generally expressed in terms of a deflection length $\lambda \approx P_b^{1/3} d^{2/3}$, which replaces the persistence length as an independent length scale (Odijk, 1983). The free energy of entropic confinement per unit length of the strand in the plectonemic supercoil may then be written approximately as (Odijk, 1983, 1993a; Helfrich and Harbich, 1985; Marko and Siggia, 1994)

$$\frac{\mathcal{F}_{conf}}{k_B T} = \frac{c_r}{P_b^{1/3} d_r^{2/3}} + \frac{c_p}{P_b^{1/3} d_p^{2/3}} \tag{24}$$

The coefficients c_r and c_p are here $3/2^{8/3}$ (we have reexamined them in Appendix I).

The undulation-enhanced free energy per unit length of strand, which is of electrostatic origin and here scaled by $k_B T$, is thus expressed as

$$f = \frac{\mathcal{F}_{el}}{k_B T} + \frac{\mathcal{F}_{conf}}{k_B T} \tag{25}$$

All terms contributing to the free energy should be averaged over the relevant semiclassical paths. The undulatory degrees of freedom of a confined worm are weighted via the

free energy of confinement; the confinement due to the electrostatic interaction is evaluated within a Gaussian approximation. In principle, the torsional forces, restraining the strands in the supercoil via White's relation (Eq. 4), should also be renormalized over all undulations. An approximate evaluation of the torsional energy, allowing for undulations that do not disrupt the plectonemic symmetry, is straightforward, but the undulatory effect turns out to be negligible. Some advances toward a more rigorous approach have been forwarded by Shimada and Yamakawa (1984, 1985), by Marko and Siggia (1995), and by Odijk (1996). However, simple quantitative approximation schemes for the coupling between torsional deformation and entropy in confined or topologically constrained systems have yet to be proposed. Moreover, the backbone of the plectoneme is not perfectly straight as assumed here, but fluctuates on length scales that are possibly on the order of the superhelical pitch, so that we may expect some influence of these fluctuations on the internal structure of the superhelix. We do not address these topics here, but simply assume that torsional effects are adequately taken into account by considering only the classical plectonemic path.

FREE ENERGY

In line with an approximate minimization procedure proposed by us (Odijk and Ubbink, 1998), we write the total free energy per unit length of strand of the plectonemic helix in the following form:

$$\frac{\mathcal{F}}{k_B T} = \mathcal{H}_c + f = \frac{1}{2} P_b \kappa_c^2 + \frac{1}{2} P_t \Omega^2 + f \qquad (26)$$

The Hamiltonian $\mathcal{H}_c$ consists of the elastic free energy of the regular plectonemic helix, and f will be assumed to be a perturbation. P_b and P_t are the persistence lengths associated with the bending and torsional deformations, respectively.

In our two-variable description in terms of the variables r and α, defined by $\tan \alpha = p/r$ (Odijk and Ubbink, 1998), the ideal plectonemic curvature κ_c and the excess twist Ω of the plectonemic helix become

$$\kappa_c = \frac{\cos^2 \alpha}{r} \quad \Omega = \frac{2\pi \Delta Tw}{l} = 2\pi \left[\frac{|\sigma|}{h} - \frac{\sin \alpha \cos \alpha}{2\pi r} \right] \qquad (27)$$

The explicit dependence of the excess twist on ΔTw has been eliminated via White's relation (Eq. 4) and the expression for the writhe (Eq. 3).

In the general case, the forces perturbing the plectonemic helix may be taken together in f, the perturbation per unit length of strand (Odijk and Ubbink, 1998). One could mention, for instance, global deformations of the plectonemic helix, external forces acting on the superhelix, interactions between the strands within the supercoil and the undulation entropy, the effects of end loops and branching points, and intersupercoil interactions between colliding superhelices in crowded states. Of course, one assumes that the perturbations are such that the postulate of a "classical" plectonemic helix remains viable.

In this paper we concentrate only on the interplay of undulation-enhanced electrostatic interaction and confinement entropy as the major force perturbing the plectonemic helix. In Appendix II we show that one other type of perturbation that is sometimes thought to have a significant effect on plectonemic structure, namely attractive dispersion forces, plays only a secondary role in the regimes focused on here.

We minimize the total free energy (Eqs. 25 and 26) according to the iterative scheme proposed in a recent paper (Odijk and Ubbink, 1998). We introduce as dimensionless variables the angle $\beta \equiv 2\alpha$ and the "inverse plectonemic parameter" $\tau \equiv h_0/4\pi r|\sigma|$. In equilibrium, the first variation in the free energy with respect to these independent variables should vanish: $\partial \mathcal{F}/\partial \beta = 0$, $\partial \mathcal{F}/\partial \tau = 0$. In general, the perturbation f may contain the auxiliary variables X_i for which we also require $\partial f/\partial X_i = 0$ for all i.

Here the auxiliary variables X_i are d_r and d_p under our assumption that these should be smaller than r and p, respectively. Minimizing $\mathcal{F}$ with respect to d_r and d_p then leads to the approximate relation

$$\left(\frac{p}{d_p}\right)^2 \kappa^2 d_r^2 \approx \left(\frac{d_p}{d_r}\right)^{2/3} \qquad (28)$$

It is immediately clear that there is trouble in trying to meet this requirement. For a typical plectonemic supercoil we have $p = \mathbb{O}(r)$ and, generally, $d_p \ll p$ and $d_r \ll r$, so that $d_r = \mathbb{O}(d_p)$. Furthermore, at high and intermediate ionic strengths, $\kappa^{-1} \ll r$, and it is likely that $\kappa d_r = \mathbb{O}(1)$. It is therefore improbable that Eq. 28 can hold for the conditions of interest to the present investigation. A full numerical minimization of $\mathcal{F}$ with respect to d_r, d_p, r, and p indeed bears out that plectonemes with $d_p \ll p$ are impossible within the context of the current theory.

Equation 28 hints at a model with $p = \mathbb{O}(d_p)$, i.e., the undulations along the plectonemic axis are not restrained by electrostatics but mainly by the plectonemic structure itself. Hence, there should be virtually no undulation enhancement of the potential along the axis of the plectoneme. We propose a revised undulation-enhanced energy instead of Eq. 23:

$$\frac{\mathcal{F}_{el}}{k_B T} = \frac{\xi^2}{2Q_B} \left[\frac{\pi}{\kappa r} \right]^{1/2} \exp[2\kappa^2 d_r^2 - 2\kappa r] Z(\mu) \qquad (29)$$

and a revised form of the undulatory free energy instead of Eq. 24:

$$\frac{\mathcal{F}_{conf}}{k_B T} = \frac{c_r}{P_b^{1/3} d_r^{2/3}} + \frac{\eta c_p}{P_b^{1/3} p^{2/3}} \qquad (30)$$

Thus, we do not introduce $G_p(u_p)$ because we assume $d_p = \mathbb{O}(p)$. The effective tube confining a strand has a diameter of

about p and not d_p, according to Eq. 30. Because the density distribution is not a Gaussian, but is somewhat flattened, we also introduce a coefficient $\eta = \mathbb{O}(1)$. We do not know its precise value, but here we simply set $\eta = 1$. The merit of Eqs. 29 and 30 will have to be borne out by experiment and simulations.

Next, our leading order approximation gives for the opening angle (Odijk and Ubbink, 1998)

$$\beta \approx \pi - 2^{1/3}\left(\frac{\partial g}{\partial \tau}\Big|_{\alpha}\right)^{1/3} \tag{31}$$

The perturbation f has been rescaled as $g \equiv 2P_b\,(h_0/2\pi P_b|\sigma|)^2 f$. The radius of the supercoil follows from the opening angle (Odijk and Ubbink, 1998):

$$\tau \approx \frac{E\sin\beta - (1/4)\sin^3\beta}{(1+\cos\beta)^2 + E\sin^2\beta} \tag{32}$$

where $E = P_t/P_b$. We stress that Eqs. 31 and 32 indicate that the opening angle will not be very sensitive to changes in the electrostatic perturbation g.

For the sake of completeness, we explicitly state the way we compute $\partial g/\partial\tau$, i.e., $\partial f/\partial\tau$. We minimize $\mathcal{F}$ with respect to d_r, which leads to

$$\frac{\partial f}{\partial d_r} = \frac{\partial(\mathcal{F}_{el} + \mathcal{F}_{conf})}{k_B T \partial d_r} = 0 \tag{33}$$

with the help of Eqs. 25, 29, and 30. Next, we define the derivatives

$$\frac{\partial f}{\partial r}\Big|_p = \frac{\partial f}{\partial d_r}\frac{\partial d_r}{\partial r} + \frac{\partial f}{\partial r}\Big|_{p,d_r} = \frac{\partial \mathcal{F}_{el}}{k_B T \partial r}\Big|_{d_r} \tag{34}$$

$$\frac{\partial f}{\partial \tau}\Big|_{\alpha} = \left[\frac{\partial f}{\partial r}\Big|_p + \tan\alpha\,\frac{\partial f}{\partial p}\Big|_r\right]\frac{\partial r}{\partial \tau}\Big|_{\alpha} \tag{35}$$

(In Eqs. 34 and 35, it is useful to reintroduce the original variables: $f = f(r, p)$). It is now straightforward to solve Eqs. 31–35 by numerical iteration.

In the next section, our undulation-enhancement theory is compared with experimental data on the basis of Eqs. 31–35. One could, of course, argue in favor of a full numerical minimization of the total free energy (Eq. 26) together with Eqs. 29 and 30 with respect to the parameters r, p (or α), and d_r. See Table 3 for a quantitative comparison of both methods: it is evident that our iterative scheme does capture the main features of the plectonemic helix in the limit of tight superhelical winding. We stress that our two-variable model is not free from limitations, but the analytical approximations, Eqs. 31 and 32, do not worsen the status of the theory, given the possible small errors incurred in the formulation of the theory from the very beginning.

DISCUSSION

Choice of parameters

The parameters that enter our theory are all known independently within rather narrow bounds. The theory is therefore essentially without any adjustable parameters. In the previous sections and in Appendix I, we have already introduced numerical values for the parameters pertaining to the characterization of the topological state and the free energy of entropic confinement, so that we are left to specify here the DNA elastic constants and the electrostatic parameters.

The DNA bending persistence length P_b is now known with reasonable accuracy. The results from a variety of experiments agree on a value of 50 nm, at high ionic strengths (Hagerman, 1988; Wang et al., 1997; Baumann et al., 1997). The assignment of a numerical value to the torsional persistence length P_t, on the other hand, is somewhat equivocal. Current experimental values may differ by about a factor of 2, the origin of the discrepancy still being a matter of some controversy (Hagerman, 1988; Schurr et al., 1992; Crothers et al., 1992; Gebe et al., 1996; Schurr, personal communication; Moroz and Nelson, 1998). Here we choose the two extremes $P_t = 50$ nm and $P_t = 100$ nm, although $P_t = 75$ nm is an often favored choice in theoretical and computer work.

The DNA molecule bears two negative charges per base pair of 0.34-nm helical rise, and the unhydrated DNA hard-core radius a is close to 1.0 nm. The Poisson-Boltzmann charge parameter ξ or, equivalently, the effective linear charge density $\nu_{eff} \equiv \xi/Q_B$ can then be evaluated (Stroobants et al., 1986) if the ionic strength of the solution is also known. We will concentrate below on the microscopy experiments by Boles et al. (1990). They have carried out their measurements at a starting temperature of 298 K, at which

TABLE 3 Comparison between the minimization of the total plectonemic free energy (Eqs. 25 and 26) following the iterative scheme (Eqs. 31 and 32) and a fully numerical minimization

	α (°)		r (nm)		d_r (nm)		$Wr/\Delta Lk$		$d_r^2\kappa/r$	
$\lvert\sigma\rvert$	num.	iterat.	num.	iterat.	num.	iterat.	num.	iterat.	num.	iterat.
0.02	62.1	48.2	19.7	22.1	3.8	4.0	0.63	0.63	0.78	0.78
0.04	66.1	59.6	6.8	7.9	1.7	2.0	0.93	0.77	0.47	0.52
0.06	66.2	61.5	4.4	4.9	1.1	1.2	0.96	0.80	0.29	0.32
0.08	65.6	61.1	3.4	3.7	0.8	0.9	0.93	0.79	0.19	0.21
0.10	64.8	60.0	2.9	3.1	0.6	0.7	0.88	0.78	0.13	0.15
0.12	64.2	58.8	2.5	2.7	0.5	0.5	0.84	0.76	0.10	0.11

Parameter values are as in Table 4. $E = 2$; $P_t = 100$ nm.

the Bjerrum length Q_B is 0.715 nm. Their aqueous buffers contain ~0.105 M monovalent salt and trace amounts of the multivalent complexing agent EDTA, which, however, as co-ion to DNA, does not have a significant impact on the double-layer electrostatics. The Debye screening length κ^{-1} is 0.94 nm, so for the effective charge parameter we obtain $\xi = 4.18$. We have collected the relevant parameters in Table 4.

Comparison with experiment and computer simulations

We are rather restricted in our choice of experimental data. One problem has been that the mesoscopic structure of the superhelix is difficult to probe in sufficient detail by most experimental techniques. On the other hand, the buffers most commonly used in microbiology are often rather complex in composition and, in many cases, contain divalent or multivalent (counter) ions. This is a complicating factor, as polyelectrolyte theory based on the Poisson-Boltzmann approximation is well established only for monovalent salt (Fixman, 1979).

At present, there are two electron-microscopic studies of DNA supercoiling that turn out to be useful in a quantitative assessment of our computations. Boles et al. (1990) have carried out an extensive investigation of plectonemic structure by conventional electron microscopy. For two sizes of circular plasmid DNA, they varied the superhelical density between -0.016 and -0.117 under controlled ionic conditions. They always observed an open, rather strongly fluctuating plectonemic helix whose radius varied as $|\sigma|^{-1}$ to a very good approximation. The writhe per added link $Wr/\Delta Lk$ had a value of ~0.72 for all values of σ and was essentially constant within the margin of experimental error.

By contrast, via cryoelectron microscopy, Bednar et al. (1994) purportedly found a collapsed plectonemic state under comparable ionic conditions. The observed superhelical diameter was close to twice the hard-core diameter of DNA. From their micrographs, we have determined the plectonemic opening angle to be around 57°, which is very close to the angle of 55° reported by Boles et al. (1990) for the open structure. However, we do not expect a collapsed state at such angles on the basis of our previous theoretical work (Odijk and Ubbink, 1998) (see Eq. 32). In this discussion, we therefore restrict ourselves to the data of Boles et al. In Appendix II, we tentatively investigate the issue of superhelical collapse by attractive dispersion forces.

TABLE 4 Parameter values used in the comparison with the experimental data of Boles et al. (1990)

DNA bending persistence length	P_b	50 nm
DNA torsional persistence length	P_t	50 nm; 100 nm
DNA hard-core radius	a	1.0 nm
Helical repeat DNA relaxed state	h	3.5 nm
Bjerrum length	Q_B	0.715 nm
Debye length	κ^{-1}	0.94 nm
Poisson-Boltzmann charge parameter	ξ	4.18
Coefficients of confinement free energy	c_p, c_r	$3/2^{8/3}$

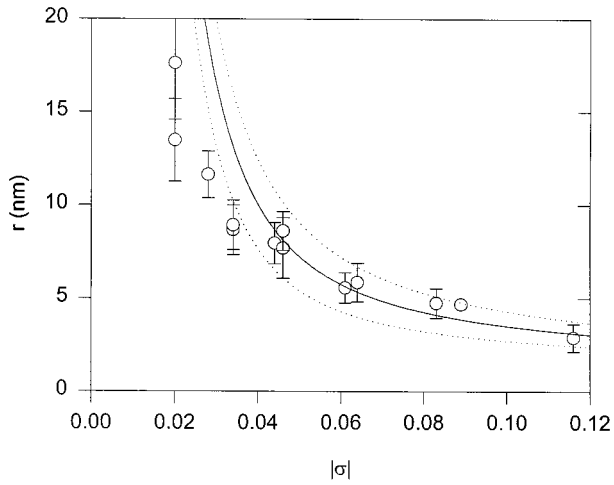

FIGURE 4 Plectonemic radius versus specific linking difference. *Circles*: Experimental data of Boles et al. (1990). The error bars indicate one standard deviation in the spread of the experimental data. *Solid line*: Theory. The dashed lines indicate the undulation amplitudes d_r. The parameters are as specified in Table 4; $P_t = 50$ nm; $E = 1$.

In Figs. 4 and 5, we plot the superhelical radius as a function of the specific linking difference for two values of the persistence ratio $E = P_t/P_b$ (see also Tables 5 and 6). Throughout the full range of σ, the agreement of theory with experiment is satisfactory for $E = 2$ but not for $E = 1$. We have also plotted the theoretical amplitudes of the undulations d_r in both figures. We observe a remarkable coincidence with the spread in experimental data, which are plotted in such a way that the error bars display one standard deviation. At low values of $|\sigma|$, the predicted amplitudes are significantly smaller than the experimental variations, even when $E = 2$. The explanation for this may be twofold. First, in this regime, our mean-field treatment of molecular fluctuations is expected to break down; specifically, the postu-

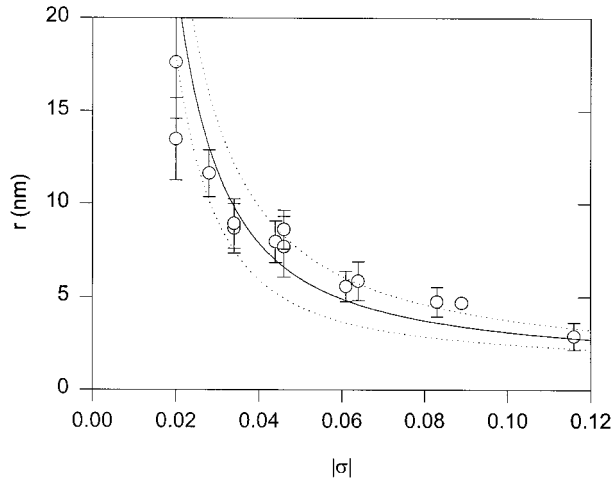

FIGURE 5 See Fig. 4, but now $P_t = 100$ nm; $E = 2$.

TABLE 5 Plectonemic parameters from the electrostatic-undulatory theory (Eqs. 31–35) for the DNA parameters quoted in Table 4

$\|\sigma\|$	α (°)	r (nm)	d_r (nm)	$Wr/\Delta Lk$	$d_r^2\kappa/r$
0.02	44.8	37.3	5.5	0.37	0.86
0.03	55.3	16.4	3.4	0.53	0.73
0.04	59.8	10.0	2.4	0.60	0.60
0.06	62.7	5.7	1.5	0.66	0.39
0.08	63.0	4.2	1.0	0.66	0.27
0.1	62.4	3.5	0.8	0.65	0.19
0.12	61.6	3.0	0.6	0.64	0.14

$P_t = 50$ nm; $E = 1$.

lated Gaussian distribution of undulations may become poor as they become too marked. Second, in the experiments at low $|\sigma|$, a regular superhelical structure will be increasingly difficult to discern, so that the distinction between regular parts of the superhelix and irregularities like branching points, end loops, and sections which are just randomly coiled becomes less clear, and, concomitantly, the margins of error will increase.

By plotting the undulation amplitudes and experimental error bars in this way, we are suggesting a direct correspondence between them, whereas the sources contributing to experimental errors may be multifarious and their relative impact difficult to gauge. For instance, it would be surprising if the handling of samples before the electron microscopic analysis did not have a significant influence on the distribution of fluctuations within the supercoil, given the highly invasive nature of the procedure. One expects strong mechanical forces to act on the supercoil, which may be flattened as it is transposed onto the EM grid. In addition, it seems difficult to maintain constant ionic conditions during this process. Furthermore, any experimental uncertainty will also be reflected in the magnitude of the error bars. Nevertheless, in view of the excellent overall agreement for $E = 2$ shown in Fig. 5, it seems reasonable to conclude that the structural fluctuations visible on the micrographs are indeed intrinsic to the superhelix in solution (Cozzarelli, personal communication).

In Fig. 6 we have plotted the normalized superhelix length as a function of the specific linking difference, again, for two values of E. This length is twice the length of the superhelical axis divided by the total contour length of the molecule. If we neglect end loops and branching points, the normalized superhelix length simply equals sin α. For convenience, nominal values of α are indicated on the axis to the right. In the experiments of Boles et al. (1990), the normalized superhelical length turns out to be effectively constant within the margin of error and is ~0.82, which implies an average opening angle of 55°. Fluctuations seem to be small but are difficult to quantify, as each measurement is the average over a considerable number of superhelical turns. An average superhelical opening angle close to 55° is obtained in a wide variety of other experiments and simulations (Adrian et al., 1990; Bednar et al., 1994; Klenin et al., 1991; Vologodskii et al., 1992). At high $|\sigma|$, our theoretical values are consistently a few degrees higher than this rather characteristic 55° (Fig. 6): both curves exhibit a broad maximum; the curve at $E = 2$ is in better agreement with experiment. Similar results, although with higher maximum values of the opening angle, were obtained in recent theoretical work (Marko and Siggia, 1994, 1995) using a superposition approximation.

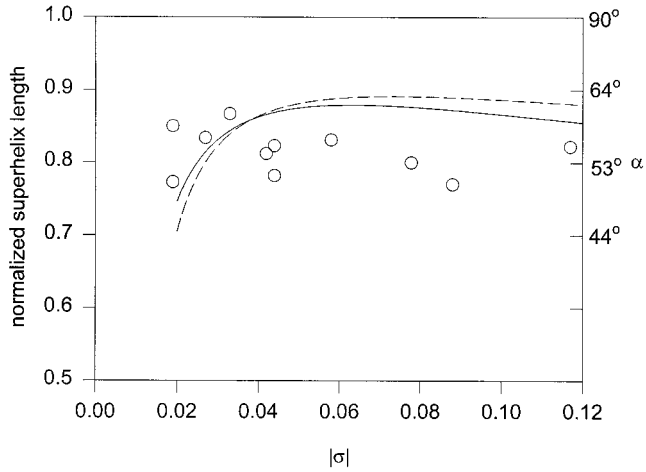

FIGURE 6 Normalized superhelix length versus specific linking difference. The nominal opening angles for an infinite plectonemic helix are indicated on the right-hand axis. *Circles*: Experimental data of Boles et al. (1990). *Dashed line*: Theory with $P_t = 50$ nm; $E = 1$. *Solid line*: Theory with $P_t = 100$ nm; $E = 2$. The parameters are as specified in Table 4.

TABLE 6 As in Table 5, but $P_t = 100$ nm, $E = 2$

$\|\sigma\|$	α (°)	r (nm)	d_r (nm)	$Wr/\Delta Lk$	$d_r^2\kappa/r$
0.02	48.2	22.1	4.0	0.63	0.79
0.03	56.2	11.8	2.7	0.73	0.65
0.04	59.6	7.9	2.0	0.77	0.52
0.06	61.5	4.9	1.2	0.80	0.32
0.08	61.1	3.7	0.9	0.79	0.21
0.1	60.0	3.1	0.7	0.78	0.15
0.12	58.8	2.7	0.5	0.76	0.11

The writhe per added link $Wr/\Delta Lk$ varies only slightly for values of $|\sigma|$ higher than ~0.04. This is in good agreement with the experimental trend (see Fig. 7). The theoretical value at $E = 2$ is ~0.77, which is a bit higher than the values obtained from experiment. The latter are scattered within a small range centered around 0.7 (Boles et al., 1990); at high $|\sigma|$, the discrepancy may be attributed, in large part, to the disparity in the respective opening angles. Note that, although the exact magnitude of the writhe is slightly off, the minimization according to Eqs. 31 and 32 gives a dependence of Wr on ΔLk that conforms closely to the linear relationship inferred from both experiment and computer simulations.

On the whole, the theory (Eqs. 31–35) with $E = 2$ is in conformity with the dimensions of superhelical DNA determined by Boles et al. (1990), except for a slight overestimation of the pitch angle α (see Figs. 5–7). Therefore, we

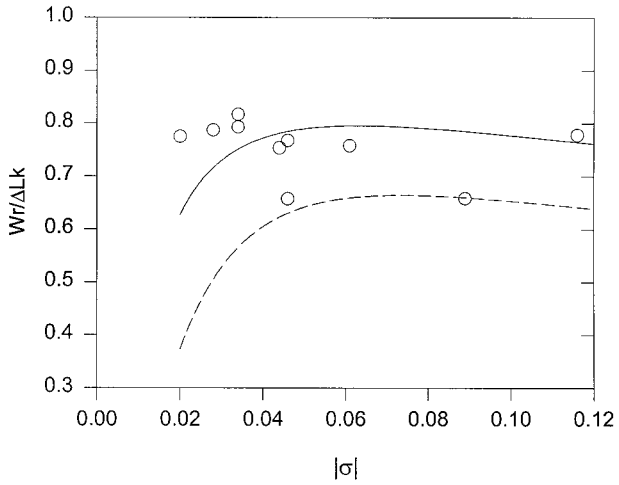

FIGURE 7 Writhe per added link versus the specific linking difference. The dashed line denotes the theory with $P_t = 50$ nm; $E = 1$. The solid line denotes the theory with $P_t = 100$ nm; $E = 2$. The open circles are the experimental data of Boles et al. (1990). The parameters are as specified in Table 4.

tend to conclude that the torsional persistence length P_t should be close to 100 nm. Such a relatively high value is in agreement with a careful theoretical treatment by Moroz and Nelson (1998). They insist on a P_t of 109 nm if they want to explain the stretching experiments by Allemand and Croquette (unpublished results), although within an essentially similar theoretical scheme somewhat lower values of P_t ($E \approx 1.4$–1.7) have also been reported (Bouchiat and Mezard, 1998). In the past, lower values for P_t have been proposed, e.g., $P_t = 80$ nm (Shimada and Yamakawa, 1985), $P_t = 50$ nm (Taylor and Hagerman, 1990; Gebe et al., 1996, and references therein), and $P_t = 75$ nm (Vologodskii and Cozzarelli, 1995). The purpose of this paper is to introduce a new supercoiling model, not to determine P_t to a high degree of precision. Nevertheless, within the context of the electrostatic analysis, a value of P_t as low as 50 nm seems quite unlikely.

At this stage, we can finally remark on the validity of the Gaussian approximation for $G_r(u_r)$ (Eq. 21). It has been argued that a Gaussian undulation theory for positionally ordered systems is only legitimate when the Gaussian distribution tapers off fast enough (Odijk, 1993c; de Vries, 1994). In our case, the probability of a test strand occupying the position of its neighbor in the supercoil must be essentially zero. In quantitative terms, we then have the condition $d^2\kappa/r \leq 1$. Table 6 shows that this requirement is indeed satisfied.

Another issue of concern is the ionic strength dependence of the plectonemic parameters. This has been investigated by numerical simulation by several groups (Vologodskii and Cozzarelli, 1995; Rybenkov et al., 1997; Delrow et al., 1997). The Vologodskii group has used a set of parameters different from that compiled in our Table 4. In particular, their torsional persistence length P_t is 75 nm ($E = 1.5$), and their DNA radius is 1.2 nm (for the "hydrated" form introduced by Stigter (1977); his electrophoretic charge instead of the actual DNA charge may also be dubious in describing static DNA configurations). The newly computed DNA charge parameter ξ agrees with that calculated by Vologodskii and Cozzarelli (1995). (Compare their Table I with our Table 7). In Table 8 we present the plectoneme parameters computed with the help of Eqs. 31–35 at a specific linking difference $|\sigma| = 0.06$. Fig. 8 shows that the analytical theory for the writhe starts to deviate from the simulations a bit at ionic strengths lower than 0.1 M. We do not have an explanation for this deviation, although it is probably systematic. The recent simulation work by Delrow et al. (1997) at $|\sigma| = 0.05$ coincides, in the main, with that of Vologodskii and Cozzarelli (1995) at $|\sigma| = 0.06$. (The change from 0.05 to 0.06 does not have a marked effect on the analytical theory; compare Table 8 with Table 9).

TABLE 7 Poisson-Boltzmann parameter ξ as chosen by Stigter (1977)

c (M)	κ^{-1} (nm)	ξ
0.01	3.04	1.38
0.02	2.15	1.93
0.05	1.36	3.03
0.1	0.961	4.37
0.2	0.680	7.16
0.5	0.430	18.6
0.75	0.351	33.4
1	0.304	54.7

Linear charge density of DNA helix ≡ electrophoretic charge density = 0.73 phosphate charges per unit length; DNA diameter $d = 2.4$ nm. ξ has been computed with the help of Philip and Wooding (1970).

The dependence of the superhelical radius on salt was studied by the Vologodskii group in yet another paper (Rybenkov et al., 1997) at a different value of $|\sigma| = 0.05$. Their results are plotted in Fig. 9 together with the radius predicted by the undulatory-electrostatic theory (see Table 9). The theory overestimates the simulations by ~15% on average, although the general form of the curve is quite well predicted. Our undulation theory explains why the usual effective diameter D_{eff} of a DNA rod (Stigter, 1977) is not at all a measure of the diameter $2r$ of a DNA plectoneme: the undulations are particularly strong at high ionic strengths, so that $2r \gg D_{eff}$ in that case.

TABLE 8 Ionic strength dependence of the plectonemic parameters calculated via the electrostatic-undulatory theory (Eqs. 31–35)

c (M)	α (°)	r (nm)	d_r (nm)	$Wr/\Delta Lk$	$d_r^2\kappa/r$
0.01	51.6	7.6	1.8	0.59	0.15
0.02	55.1	6.8	1.7	0.64	0.19
0.05	59.2	5.8	1.4	0.70	0.27
0.1	61.6	5.2	1.3	0.74	0.34
0.2	63.3	4.9	1.2	0.76	0.41
0.5	64.5	4.6	1.0	0.78	0.51
0.75	64.7	4.6	0.9	0.78	0.54
1	64.8	4.6	0.9	0.79	0.57

Specific linking difference $|\sigma| = 0.06$.

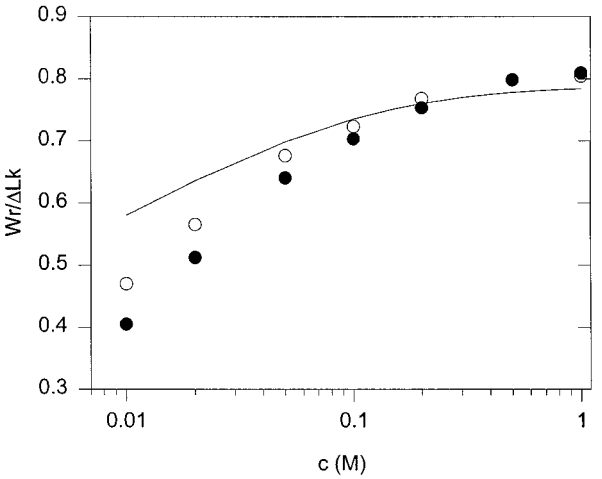

FIGURE 8 Writhe per added link as a function of the concentration of monovalent salt. Comparison between the electrostatic-undulatory theory (Eqs. 31–35) (*solid line*) and simulations by Vologodskii and Cozzarelli (1995), using either a line charge approximation to the Poisson-Boltzmann equation (*open circles*) or an effective diameter (*filled circles*). $P_t = 75$ nm ($E = 1.5$), $|\sigma| = 0.06$; electrostatic parameters are as in Table 7.

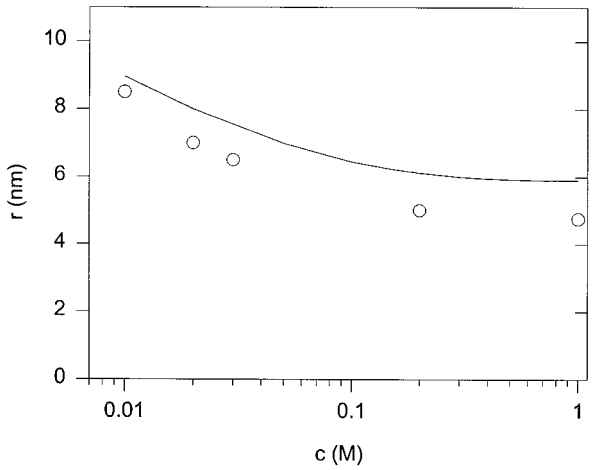

FIGURE 9 Plectonemic radius versus the concentration of monovalent salt. The open circles are from the simulations by Rybenkov et al. (1997); the solid line is the electrostatic-undulatory theory (Eqs. 31–35). $P_t = 75$ nm, $|\sigma| = 0.05$; electrostatic parameters are as in Table 7.

Finally, we emphasize that a superposition formula like Eq. 17, when enhanced by Gaussian fluctuations (Eq. 21), is not at all able to explain the ionic strength dependence of the plectoneme dimensions. We have found that such an undulatory potential leads to a virtually constant radius and writhe, in stark disagreement with Figs. 8 and 9. What happens is that the minute term $\exp[-\pi p]$ is blown up disproportionately when a Gaussian is applied. As we have argued at length, the p dependence should be accounted for to a far better degree (see Eq. 18).

CONCLUDING REMARKS

In conclusion, we have shown that, despite the seemingly fairly wild fluctuations in structure, the plectonemic helix may behave like a rather well-ordered system with respect to the radial organization of the strands within the supercoil. In the limit of tight winding, the radial undulations of the strands are small and may be dealt with on a mean-field level. By contrast, we have argued that the longitudinal fluctuations within the supercoil related to the pitch are relatively large. We have carried out a quantitative analytical computation for a plectonemic supercoil immersed in an aqueous solution containing excess monovalent salt. The undulatory electrostatics is the dominant force, and the predicted supercoil structure and undulation amplitudes of the strands agree well with current experimental data if we let the torsional persistence length be 100 nm. The special symmetry inherent in the purely elastic energy is the cause of the remarkable invariance of the plectonemic opening angle under conditions where the superhelical radius varies by almost one order of magnitude. We suspect that this effective conservation of opening angle could well have important biological consequences (Odijk, 1998).

TABLE 9 As in Table 8, but with $|\sigma| = 0.05$

c (M)	α (°)	r (nm)	d_r (nm)	$Wr/\Delta Lk$	$d_r^2\kappa/r$
0.01	52.2	9.0	2.3	0.60	0.19
0.02	55.5	8.0	2.1	0.65	0.25
0.05	59.1	7.0	1.8	0.70	0.34
0.1	61.1	6.4	1.7	0.73	0.42
0.2	62.3	6.1	1.4	0.75	0.50
0.5	63.0	5.9	1.2	0.76	0.60
0.75	63.1	5.9	1.1	0.76	0.63
1	63.1	5.9	1.1	0.76	0.65

Finally, a referee has invited us to comment on the status of the present theory and supercoiling models in general. First, it is well to recall that biophysical modeling itself is subject to an almost inexorable conflict between biological contingency and physical universality (for some general remarks on the formulation of mesoscopic models of complex matter, see Odijk (1997)). There are at least two major problems in developing a theory of DNA supercoils. The first is how to reckon with the topological constraint (the DNA helix cannot intersect itself); the second is the inevitable reduction in the number of degrees of freedom as one defines a model for real DNA in aqueous buffer (i.e., the molecule DNA surrounded by water molecules, ions, etc.). For instance, in this paper we have introduced a two-variable description of a superhelix without end effects. The supposition has been made that the DNA configurations are purely plectonemic; hence, the phase space of all possible configurations has been severely restricted. In particular, we have not introduced a reference state. Moreover, the aqueous electrolytic environment is dealt with merely at the level of Poisson-Boltzmann electrostatics. The bending and twisting degrees of freedom are purely elastic.

Another difficulty is the status of mean-field theories guided by variational principles using trial functions. For a complex system, we may devise a reasonable mathematical

model that seems to work admirably but could well turn out to be wrong in the long run (for instance, Anderson (1984) has criticized current semiempirical quantum-chemical models of complex molecules described in terms of a large set of trial functions). In any event, we have here attempted to formulate a convenient mesoscopic form of the free energy of a plectonemic supercoil. Gaining insight into the nature of the entropy, which has implicit contributions within the bending, twisting, and electrostatic parameters, is another matter.

APPENDIX I: ENTROPY OF GENERALIZED WORMLIKE CHAINS RESTRICTED TO A GAUSSIAN

Certain functional integrals related to the statistical mechanics of "generalized" wormlike chains have been investigated in some detail recently (Kleinert, 1996, 1990; Dodonov et al., 1991; Burkhardt, 1995; Jain and Nelson, 1995). However, it is possible to derive the value of an important coefficient by a simple scaling argument.

Let us consider a quadratic Hamiltonian signifying a harmonically confined "generalized" polymer:

$$\mathcal{H} \equiv \mathcal{H}_0 + U \equiv \tfrac{1}{2} g \int_0^l \mathrm{d}s \left(\frac{d^n x}{ds^n}\right)^2 + \tfrac{1}{2} b \int_0^l \mathrm{d}s x^2 \qquad (36)$$

(n = integer).

A configuration of the chain describes a one-dimensional path $x = x(s)$. The partition function is defined on the space of paths $[x(s)]$. The harmonic potential U of strength b has been added to the "bending" term $\mathcal{H}_0$. This simulates the effect of constraining the chain to a Gaussian distribution (as $l \to \infty$):

$$G(x) = \frac{1}{\pi^{1/2} d} \exp\left[-\frac{x^2}{d^2}\right] \qquad (37)$$

The fully quadratic form of Eq. 36 ensures that the simulated distribution is exactly Gaussian.

Next, assume that a deflection length λ exists. Estimates for the energy scales are simply

$$\mathcal{H}_0 \approx \frac{g l d^2}{\lambda^{2n}} \qquad (38)$$

$$U \approx b l d^2 \qquad (39)$$

so that a balance of these two terms implies

$$\lambda \approx (g/b)^{1/2n} \qquad (40)$$

The chain is a sequence of deflection segments, so the total free energy, which is extensive, is given by

$$F_{\mathrm{tot}} \approx \frac{l}{\lambda} \approx l \left(\frac{b}{g}\right)^{1/2n} \qquad (l \gg \lambda) \qquad (41)$$

Furthermore, Eq. 36 together with the standard definition of the partition function gives the average potential:

$$\langle U \rangle = b \frac{\partial F_{\mathrm{tot}}}{\partial b} = \frac{1}{2n} F_{\mathrm{tot}} \qquad (42)$$

Finally, to focus on the correct expression for the free energy of confining the polymer in accordance with the restriction in Eq. 37, we have to acknowledge that the external potential U is merely an artifice (Odijk, 1986):

$$F_{\mathrm{conf}} \equiv F_{\mathrm{tot}} - \langle U \rangle = \left(1 - \frac{1}{2n}\right) F_{\mathrm{tot}} \qquad (43)$$

The coefficient $(1 - 1/2n)$ is in agreement with computations for $n = 1$ (Odijk, 1986) and $n = 2$ (Kleinert, 1986; Burkhardt, 1995). If the chain were to be viewed as an effective harmonic oscillator, the coefficient would be 1/2 (Odijk, 1986), but for the system at hand ($n = 2$), such a point of view is incorrect. Care must also be exercised in applying a virial theorem (Landau and Lifshitz, 1976) to Eq. 36. To sum up, for a one-dimensional worm ($n = 2$, $g \equiv P_{\mathrm{b}} k_{\mathrm{B}} \mathrm{T}$) Eq. 43 still holds, so we have (Burkhardt, 1995)

$$\frac{\mathcal{F}_{\mathrm{conf}}}{k_{\mathrm{B}} T} = \frac{3}{2^{8/3} P_{\mathrm{b}}^{1/3} d^{2/3}} \qquad (44)$$

APPENDIX II: INFLUENCE OF WEAK ATTRACTIVE INTERACTIONS ON PLECTONEMIC STRUCTURE

In cryoelectron microscopic studies, collapsed states of plectonemically supercoiled DNA have purportedly been witnessed in which the two strands of a supercoil had adhered laterally (Bednar et al., 1994). The collapse was observed at a specific linking difference of about -0.05 in buffers containing either 0.1 M NaCl or 0.01 M $MgCl_2$.

Under these ionic conditions, one would ordinarily assume the usual electrostatic repulsion to dominate any attractive interaction between DNA segments. However, there is evidence that nonsupercoiled DNA aggregates at high enough DNA concentrations (Wissenburg et al., 1994, 1995). Nevertheless, the aggregation has been thought to arise from attractive forces at the third virial level, i.e., beyond the pair level (Odijk, 1994; Wissenburg et al., 1995). There may be little or no relation between the two sets of experiments, after all (Bednar et al., 1994; Wissenburg et al., 1994, 1995).

In recent years, the origin and role of attractive interactions in colloidal and polymer solutions have become a matter of some debate. At present, short-range ion-ion correlation forces (Oosawa, 1968; Schmitz, 1996; Rouzina and Bloomfield, 1996; Grønbech-Jensen et al., 1997) and an exponentially decaying long-range attraction, of unknown but possibly hydrophobic nature (Odijk, 1994), are thought to compete in strength with the classical London-Hamaker interaction. In this appendix, we do not enter into this debate and simply gauge the effect of one type of attractive interaction on plectonemic structure, namely dispersion forces. These are weak, of course, but the twisting force within supercoiled DNA brings about an additional interaction pulling the strands of the plectoneme together. It is worthwhile to investigate whether both effects in concert could induce side-by-side adhesion. A rough calculation was performed recently (Marko and Siggia, 1995), but, as explained in the Introduction, we go somewhat deeper into several issues here.

In the nonretarded regime, the van der Waals interaction between a volume element $\mathrm{d}V_1$ of the test strand of the supercoil and a volume element $\mathrm{d}V_2$ of the opposing strand may be written as $A k_{\mathrm{B}} T / \rho^6 \, \mathrm{d}V_1 \, \mathrm{d}V_2$, where A is the Hamaker constant scaled by $k_{\mathrm{B}} T$ and ρ is the distance between $\mathrm{d}V_1$ and $\mathrm{d}V_2$ (Derjaguin, 1989). Only the strand opposing the test strand contributes significantly to the van der Waals free energy because the force is short-ranged.

Both the radius and the pitch of the superhelix are much larger than the DNA hardcore radius a, so we may approximate a volume element of strand by $\mathrm{d}V = \pi a^2 \mathrm{d}s$, where $\mathrm{d}s$ is an element of length along a superhelical strand. We neglect the variation in the van der Waals forces across the cross section of the DNA double helix, which would give rise to a correction of relative magnitude $\mathbb{O}(a^2/r^2)$ to the total interaction (Sparnaay, 1959).

The van der Waals forces are only weakly perturbed by undulations, at least within the Gaussian approximation (Odijk, 1993b). Hence we neglect this undulatory correction also; so we calculate the interaction as if the

DNA strands were in their classical plectonemic configuration (Fig. 1). A volume element of strand is written as $dV = \pi a^2[p^2 + r^2]^{1/2}\, du \cdot \rho(u) = [2r^2[1 + \cos(u)] + p^2u^2]^{1/2}$, where u is the parameterization along the plectonemic axis introduced earlier (see also Fig. 2).

The free energy of attraction per unit length of strand in the plectonemic helix thus becomes

$$\frac{\mathcal{F}_{\mathrm{VdW}}}{k_{\mathrm{B}}T} = -Aa^4[p^2 + r^2]^{1/2} \int_{-\infty}^{\infty} du\, \frac{1}{\rho(u)^6} \qquad (45)$$

We anticipate that $p > r$, so that we may approximate $\rho(u) \approx [4r^2 + p^2u^2]^{1/2}$. Accordingly, we obtain

$$\frac{\mathcal{F}_{\mathrm{VdW}}}{k_{\mathrm{B}}T} \approx -\frac{3\pi Aa^4}{256}\frac{[p^2 + r^2]^{1/2}}{r^5 p} = -\frac{3\pi Aa^4}{256 r^5 \sin\alpha} \qquad (46)$$

We minimize the total free energy of the supercoil according to the iterative scheme in Eqs. 31 and 32. The perturbation per unit length of strand now consists of the electrostatic undulatory interaction plus the van der Waals free energy:

$$f = \frac{\mathcal{F}_{\mathrm{el}}}{k_{\mathrm{B}}T} + \frac{\mathcal{F}_{\mathrm{conf}}}{k_{\mathrm{B}}T} + \frac{\mathcal{F}_{\mathrm{VdW}}}{k_{\mathrm{B}}T} \qquad (47)$$

The effect of the van der Waals interaction is largest when r is as small as possible. We therefore merely regard the case in which the absolute linking difference is the maximum attained in the experiments by Boles et al. (1990), namely, $|\sigma| = 0.12$. Then we have

$$\frac{\mathcal{F}_{\mathrm{VdW}}}{\mathcal{F}_{\mathrm{el}}} = -\mathbb{O}(A/1000) \qquad (48)$$

DNA in water should have a scaled Hamaker constant of order unity; it is clear that the dispersion interaction is entirely negligible. Furthermore, it turns out that the secondary minimum we are focusing on is separated from the totally collapsed state (when the two strands adhere) by a huge energy barrier of $\sim 20 k_{\mathrm{B}}T$/nm strand.

In addition, we note that the opening angle as determined by us from the electron micrographs of Bednar et al. (1994) is ~57°, which is close to the 55° obtained by Boles et al. (1990) for the open structures. As we have stressed earlier, the combination of a very slight variation in the opening angle versus a huge variation in the superhelical radius as in a collapsed state contradicts our semiclassical relation (Eq. 32). The contradiction hints at an inconsistency in the experimental data. Gebe et al. (1996) recently presented arguments for why the collapsed state of the plectonemic superhelix seen by Bednar et al. (1994) may actually be an artifact of the vitrification procedure used in cryoelectron microscopy.

We thank J. Bednar, J. Langowski, and C. L. Woldringh for discussions and especially N. R. Cozzarelli and J. M. Schurr for very helpful comments.

We gratefully acknowledge financial support from the Netherlands Foundation for Chemical Research (SON).

REFERENCES

Adrian, M., B. Ten Heggeler-Bordier, W. Wahli, A. Z. Stasiak, A. Stasiak, and J. Dubochet. 1990. Direct visualization of supercoiled DNA molecules in solution. *EMBO J.* 9:4551–4554.

Anderson, P. W. 1984. Basic Notions of Condensed Matter Physics. Benjamin-Cummings, Menlo Park, CA.

Bates, A. D., and A. Maxwell. 1993. DNA Topology. IRL Press, Oxford.

Bauer, W., F. H. C. Crick, and J. H. White. 1978. Supercoiled DNA. *Sci. Am.* 243:100–113.

Bauer, W., and J. Vinograd. 1970. Interaction of closed circular DNA with intercalative dyes. II. The free energy of superhelix formation in SV40 DNA. *J. Mol. Biol.* 47:419–435.

Baumann, C. G., S. B. Smith, V. A. Bloomfield, and C. Bustamente. 1997. Ionic effects on the elasticity of single DNA molecules. *Proc. Natl. Acad. Sci. USA.* 94:6185–6190.

Bednar, J., P. Furrer, A. Stasiak, J. Dubochet, E. H. Egelman, and A. D. Bates. 1994. The twist, writhe and overall shape of supercoiled DNA change during counterion-induced transition from a loosely to a tightly interwound superhelix. *J. Mol. Biol.* 235:825–847.

Bender, C. M., and S. A. Orszag. 1978. Advanced Mathematical Methods for Scientists and Engineers. McGraw-Hill, Singapore.

Benham, C. J. 1979. An elastic model of the large-scale structure of duplex DNA. *Biopolymers.* 18:609–623.

Benham, C. J. 1983. Geometry and mechanics of DNA superhelicity. *Biopolymers.* 22:2477–2495.

Benham, C. J. 1990. Theoretical analysis of heteropolymeric transitions in superhelical DNA molecules of specified sequence. *J. Chem. Phys.* 92:6294–6305.

Bloomfield, V. A., D. M. Crothers, and I. Tinoco. 1974. Physical Chemistry of Nucleic Acids. Harper and Row, New York.

Boles, T. C., J. H. White, and N. R. Cozzarelli. 1990. Structure of plectonemically supercoiled DNA. *J. Mol. Biol.* 213:931–951.

Bouchiat, C., and M. Mezard. 1998. Elasticity model of a supercoiled DNA molecule. *Phys. Rev. Lett.* 80:1556–1559.

Brady, G. W., D. B. Fein, H. Lambertson, V. Grassian, D. Foos, and C. J. Benham. 1987. X-ray scattering from the superhelix in circular DNA. *Proc. Natl. Acad. Sci. USA.* 80:741–744.

Brenner, S. L., and V. A. Parsegian. 1974. A physical method for deriving the electrostatic interaction between rodlike polyions at all mutual angles. *Biophys. J.* 14:327–334.

Burkhardt, T. W. 1995. Free energy of a semiflexible polymer confined along an axis. *J. Phys. A Math. Gen.* 28:L629–L635.

Călugăreanu, G. 1959. Sur les classes d'isotopie des noeuds tridimensionnels et leurs invariants. *Czech. Math. J.* 11:588–624.

Camerini-Otero, R. D., and G. Felsenfeld. 1978. A simple model of DNA superhelices in solution. *Proc. Natl. Acad. Sci. USA.* 75:1708–1712.

Chirico, G., U. Kapp, K. Klenin, W. Kremer, and J. Langowski. 1993. Ten microseconds in the life of a superhelix. *J. Math. Chem.* 13:33–43.

Cozzarelli, N. R., T. C. Boles, and J. H. White. 1990. Primer on the topology and geometry of DNA supercoiling. *In* DNA Topology and Its Biological Effects. N. R. Cozzarelli and J. C. Wang, editors. Cold Spring Harbor Laboratory Press, Cold Spring Harbor, NY. 139–184.

Cozzarelli, N. R., and J. C. Wang. 1990. DNA Topology and Its Biological Effects. Cold Spring Harbor Laboratory Press, Cold Spring Harbor, NY.

Crothers, D. M., J. Drak, J. D. Kahn, and S. D. Levene. 1992. DNA bending, flexibility, and helical repeat by cyclization kinetics. *Methods Enzymol.* 212:2–29.

Delrow, J. J., J. A. Gebe, and J. M. Schurr. 1997. Comparison of hard-cylinder and screened Coulomb interactions in the modeling of supercoiled DNAs. *Biopolymers.* 42:455–470.

Depew, R. E., and J. C. Wang. 1975. Conformational fluctuations of DNA helix. *Proc. Natl. Acad. Sci. USA.* 72:4275–4279.

Derjaguin, B. V. 1989. Theory of the Stability of Colloids and Thin Films. Consultants Bureau, New York.

de Vries, R. 1994. Undulation-enhanced electrostatic forces in lamellar phases of fluid membranes. *J. Phys. II.* 4:1541–1555.

Dodonov, V. V., A. B. Klimov, and V. I. Man'ko. 1991. Exact propagators for Lagrangians with higher derivatives in quantum mechanics. *Physica A.* 170:595–611.

Drew, H. R., J. R. Weeks, and A. A. Travers. 1985. Negative supercoiling induces spontaneous unwinding of a bacterial promoter. *EMBO J.* 4:1025–1032.

Fenley, M. O., W. K. Olson, I. Tobias, and G. S. Manning. 1994. Electrostatic effects in short superhelical DNA. *Biophys. Chem.* 50:255–271.

Fixman, M. 1979. The Poisson-Boltzmann equation and its application to polyelectrolytes. *J. Chem. Phys.* 70:4995–5005.

Fixman, M. 1982. The flexibility of polyelectrolyte molecules. *J. Chem. Phys.* 76:6346–6353.

Fuller, F. B. 1971. The writhing number of a space curve. *Proc. Natl. Acad. Sci. USA.* 68:815–819.

Fuller, F. B. 1978. Decomposition of the linking number of a closed ribbon: a problem from molecular biology. *Proc. Natl. Acad. Sci. USA.* 75:3557–3561.

Gebe, J. A., J. J. Delrow, P. J. Heath, B. S. Fujimoto, D. W. Stewart, and J. M. Schurr. 1996. Effects of Na^+ and Mg^{2+} on the structures of supercoiled DNAs: comparison of simulations with experiments. *J. Mol. Biol.* 262:105–128.

Gellert, M. 1981. DNA topoisomerases. *Annu. Rev. Biochem.* 50:879–910.

Gellert, M., and H. Nash. 1987. Communication between segments of DNA during site-specific recombination. *Nature.* 235:401–404.

Grønbech-Jensen, N., R. J. Mashl, R. F. Bruinsma, and W. M. Gelbart. 1997. Counterion-induced attraction between rigid polyelectrolytes. *Phys. Rev. Lett.* 78:2477–2480.

Guitter, E., and S. Leibler. 1992. On supercoiling instability in closed DNA. *Europhys. Lett.* 17:643–648.

Hagerman, P. J. 1988. Flexibility of DNA. *Annu. Rev. Biophys. Biophys. Chem.* 17:265–286.

Hao, M.-H., and W. K. Olson. 1989. Global equilibrium configurations of supercoiled DNA. *Macromolecules.* 22:3292–3303.

Hearst, J. E., and N. G. Hunt. 1991. Statistical mechanical theory for the plectonemic DNA supercoil. *J. Chem. Phys.* 95:9322–9328.

Helfrich, W., and W. Harbich. 1985. Adhesion and cohesion of tubular vesicles. *Chem. Scripta.* 25:32–36.

Hsieh, T., and J. C. Wang. 1975. Thermodynamic properties of superhelical DNAs. *Biochemistry.* 14:527–535.

Hunt, N. G., and J. E. Hearst. 1991. Elastic model of DNA supercoiling in the infinite-length limit. *J. Chem. Phys.* 95:9329–9336.

Jain, S., and D. R. Nelson. 1996. Icelike melting of hexagonal columnar crystals. *Macromolecules.* 29:8523–8529.

Keller, W. 1975. Determination of the number of superhelical turns in simian virus 40 DNA by gel electrophoresis. *Proc. Natl. Acad. Sci. USA.* 72:4876–4880.

Keller, W., and I. Wendel. 1974. Stepwise relaxation of supercoiled SV40 DNA. *Cold Spring Harb. Symp. Quant. Biol.* 39:199–208.

Kleinert, H. 1986. Path integral for second-derivative Lagrangian $L = (\kappa/2)\ddot{x} + (m/2)\dot{x}^2 + (k/2)x^2 - j(\tau)x(\tau)$. *J. Math. Phys.* 27:3003–3013.

Kleinert, H. 1990. Path Integrals in Quantum Mechanics, Statistics and Polymer Physics, 2nd ed. World Scientific, Singapore.

Klenin, K. V., A. V. Vologodskii, V. V. Anshelevich, A. M. Dykhne, and M. D. Frank-Kamenetskii. 1991. Computer simulation of DNA supercoiling. *J. Mol. Biol.* 217:413–419.

Landau, L. D., and E. M. Lifshitz. 1976. Mechanics, 3rd ed. Pergamon Press, Oxford.

Langowski, J., W. Kremer, and U. Kapp. 1990. Dynamic light scattering for study of solution conformation of superhelical DNA. *Methods Enzymol.* 211:430–448.

Le Bret, M. 1979. Catastrophic variation of twist and writhing of circular DNAs with constraint? *Biopolymers.* 18:1709–1725.

Le Bret, M. 1984. Twist and writhing in short circular DNAs according to first-order elasticity. *Biopolymers.* 23:1835–1867.

Liu, L. F., L. Perkocha, R. Calendar, and J. C. Wang. 1981. Knotted DNA from bacteriophage capsids. *Proc. Natl. Acad. Sci. USA.* 78:5498–5502.

Liu, L. F., and J. C. Wang. 1987. Supercoiling of the DNA template during transcription. *Proc. Natl. Acad. Sci. USA.* 84:7024–7027.

Marko, J. F., and E. D. Siggia. 1994. Fluctuations and supercoiling of DNA. *Science.* 265:506–508.

Marko, J. F., and E. D. Siggia. 1995. Statistical mechanics of supercoiled DNA. *Phys. Rev. E.* 52:2912–2938.

Martin, K., and J. C. Wang. 1970. Electron microscopic studies of topologically interlocked λb2b5c DNA rings. *Biopolymers.* 9:503–505.

Moroz, J. D., and P. Nelson. 1998. Entropic elasticity of twist-storing polymers. *Macromolecules.* 31:6333–6347.

Odijk, T. 1983. On the statistics and dynamics of confined or entangled stiff polymers. *Macromolecules.* 16:1340–1344.

Odijk, T. 1986. Theory of lyotropic polymer liquid crystals. *Macromolecules.* 19:2313–2328.

Odijk, T. 1993a. Undulation-enhanced electrostatic interaction in hexagonal polyelectrolyte gels. *Biophys. Chem.* 46:69–75.

Odijk, T. 1993b. Undulation-enhanced forces in hexagonal gels of semiflexible polyelectrolytes. *ACS Symp. Ser.* 548:86–97.

Odijk, T. 1993c. Evidence for undulation-enhanced electrostatic forces from the melting curves of a lamellar phase and a hexagonal polyelectrolyte gel. *Europhys. Lett.* 24:177–182.

Odijk, T. 1994. Long-range attraction in polyelectrolyte solutions. *Macromolecules.* 27:4998–5003.

Odijk, T. 1996. DNA in a liquid-crystalline environment: tight bends, rings, supercoils. *J. Chem. Phys.* 106:1270–1286.

Odijk, T. 1997. Ilya M. Lifshitz. An appreciation. *Phys. Rep.* 288:9–12.

Odijk, T. 1998. Osmotic compaction of supercoiled DNA into a bacterial nucleoid. *Biophys. Chem.* 73:23–29.

Odijk, T., and J. Ubbink. 1998. Dimensions of a plectonemic DNA supercoil under fairly general perturbations. *Physica A.* 252:61–66.

Olson, W. K., and P. Zhang. 1991. Computer simulation of DNA supercoiling. *Methods Enzymol.* 203:403–433.

Olver, F. W. J. 1974. Asymptotics and Special Functions. Academic Press, New York.

Onsager, L. 1949. The effects of shape on the interaction of colloidal particles. *Ann. N.Y. Acad. Sci.* 51:627–659.

Oosawa, F. 1968. Interaction between parallel rodlike macroions. *Biopolymers.* 6:1633–1647.

Philip, J. R., and R. A. Wooding. 1970. Solution of the Poisson-Boltzmann equation about a cylindrical particle. *J. Chem. Phys.* 52:953–959.

Pulleyblank, D. E., M. Shure, D. Tang, J. Vinograd, and H. P. Vosberg. 1975. Action of nicking-closing enzyme on supercoiled and nonsupercoiled closed circular DNA: formation of a Boltzmann distribution of topological isomers. *Proc. Natl. Acad. Sci. USA.* 72:4280–4284.

Rouzina, I., and V. A. Bloomfield. 1996. Macroion attraction due to electrostatic correlation between screening counterions. 1. Mobile surface-adsorbed ions and diffusive ion cloud. *J. Phys. Chem.* 100: 9977–9989.

Rybenkov, V. V., A. V. Vologodskii, and N. R. Cozzarelli. 1997. The effect of ionic conditions on the conformations of supercoiled DNA. I. Sedimentation analysis. *J. Mol. Biol.* 267:299–311.

Schmitz, K. S. 1996. On the "attractive component" to the free energy of interaction between macroions of like charge. *Acc. Chem. Res.* 29:7–11.

Schurr, J. M., B. S. Fujimoto, P. Wu, and L. Song. 1992. Fluorescence studies of nucleic acids: dynamics, rigidities, and structures. *In* Topics in Fluorescence Spectroscopy, Vol. 3, Biochemical Applications. J. R. Lakowics, editor. Plenum Press, New York. 137–229.

Seidl, A., and H.-J. Hinz. 1984. The free energy of DNA supercoiling is enthalpy-determined. *Proc. Natl. Acad. Sci. USA.* 81:1312–1316.

Shi, Y., and J. E. Hearst. 1994. The Kirchhoff elastic rod, the nonlinear Schrödinger equation, and DNA supercoiling. *J. Chem. Phys.* 101: 5186–5199 (Erratum *J. Chem. Phys.* 109:2959–2961 (1998)).

Shimada, J., and H. Yamakawa. 1984. Ring-closure probabilities for twisted worm-like chains. Application to DNA. *Macromolecules.* 17: 689–698.

Shimada, J., and H. Yamakawa. 1985. Statistical mechanics of DNA topoisomers. *J. Mol. Biol.* 184:319–329.

Shore, D., and R. L. Baldwin. 1983. Energetics of DNA twisting. I. Relation between twist and cyclization probability. *J. Mol. Biol.* 170: 957–981.

Shore, D., J. Langowski, and R. L. Baldwin. 1981. DNA flexibility studied by covalent closure of short fragments into circles. *Proc. Natl. Acad. Sci. USA.* 78:4833–4837.

Sinden, R. R. 1987. Supercoiled DNA: biological significance. *J. Chem. Educ.* 64:294–301.

Sinden, R. R. 1994. DNA Structure and Function. Academic Press, San Diego.

Sparnaay, M. J. 1959. The interaction between two cylinder shaped colloidal particles. *Rec. Trav. Chim. Pays-Bays.* 78:680–709.

Stasiak, A. 1996. Circular DNA. *In* Large Ring Molecules. J. A. Semlyen, editor. Wiley, Chichester. 43–97.

Stigter, D. 1977. Interactions of highly charged colloidal cylinders with applications to double stranded DNA. *Biopolymers.* 16:1435–1448.

Strick, T. R., J.-F. Allemand, D. Bensimon, A. Bensimon, and V. Croquette. 1996. The elasticity of a single supercoiled DNA molecule. *Science.* 271:1835–1837.

Stroobants, A., H. N. W. Lekkerkerker, and T. Odijk. 1986. Effect of electrostatic interaction on the liquid crystal phase transition of rodlike polyelectrolytes. *Macromolecules.* 19:2232–2238.

Tanaka, F., and H. Takahashi. 1985. Elastic theory of supercoiled DNA. *J. Chem. Phys.* 83:6017–6026.

Taylor, W. H., and P. J. Hagerman. 1990. Application of the method of phage T4 DNA ligase-catalyzed ring-closure to the study of DNA structure. II. Sodium chloride-dependence of DNA flexibility and helical repeat. *J. Mol. Biol.* 212:363–376.

Tsuru, H., and M. Wadati. 1986. Elastic model of highly supercoiled DNA. *Biopolymers.* 25:2083–2096.

Vinograd, J., J. Lebowitz, R. Radloff, R. Watson, and P. Laipis. 1965. The twisted circular form of polyoma viral DNA. *Proc. Natl. Acad. Sci. USA.* 53:1104–1111.

Vologodskii, A. V., V. V. Anshelevich, A. V. Lukashin, and M. D. Frank-Kamenetskii. 1979. Statistical mechanics of supercoils and the torsional stiffness of the DNA double helix. *Nature.* 280:294–298.

Vologodskii, A. V., and N. R. Cozzarelli. 1995. Modeling of long-range electrostatic interactions in DNA. *Biopolymers.* 35:289–296.

Vologodskii, A. V., S. D. Levene, K. V. Klenin, M. Frank-Kamenetskii, and N. R. Cozzarelli. 1992. Conformational and thermodynamic properties of supercoiled DNA. *J. Mol. Biol.* 227:1224–1243.

Wadati, M., and H. Tsuru. 1986. Elastic model of looped DNA. *Physica.* 21D:213–226.

Wang, J. C. 1971. Interaction between DNA and an *Escherichia coli* protein *ω*. *J. Mol. Biol.* 55:523–533.

Wang, J. C. 1991. DNA topoisomerases: why so many? *J. Biol. Chem.* 266:6659–6662.

Wang, J. C. 1996. DNA topoisomerases. *Annu. Rev. Biochem.* 65: 635–692.

Wang, M. D., H. Yin, R. Landick, J. Gelles, and S. M. Block. 1997. Stretching DNA with optical tweezers. *Biophys. J.* 72:1335–1346.

Wasserman, S. A., and N. R. Cozzarelli. 1986. Biochemical topology: applications to DNA recombination and replication. *Science.* 232: 951–960.

Westcott, T. P., I. Tobias, and W. K. Olson. 1997. Modeling self-contact forces in the elastic theory of DNA supercoiling. *J. Chem. Phys.* 107: 3967–3980.

White, J. H. 1969. Self-linking and the Gauss integral in higher dimensions. *Am. J. Math.* 91:693–728.

White, J. H., and W. R. Bauer. 1986. Calculation of the twist and writhe for representative models of DNA. *J. Mol. Biol.* 198:329–341.

Wissenburg, P., T. Odijk, P. Cirkel, and M. Mandel. 1994. Multimolecular aggregation in concentrated isotropic solutions of mononucleosomal DNA in 1 M sodium chloride. *Macromolecules.* 27:306–308.

Wissenburg, P., T. Odijk, P. Cirkel, and M. Mandel. 1995. Multimolecular aggregation of mononucleosomal DNA in concentrated isotropic solution. *Macromolecules.* 28:2315–2328.

Wolffe, A. 1992. Chromatin Structure and Function. Academic Press, London.